AD_____

Award Number: DAMD17-02-C-0091

TITLE: Use of Epidermolysis Bullosa Biomarkers in Models of Vesicant Injury

PRINCIPAL INVESTIGATOR: Donald R. Gerecke, Ph.D.

CONTRACTING ORGANIZATION: Rutgers the State University of New Jersey
Piscataway, New Jersey 08854-8010

REPORT DATE: September 2006

TYPE OF REPORT: Final

PREPARED FOR: U.S. Army Medical Research and Materiel Command
Fort Detrick, Maryland 21702-5012

REPORT DOCUMENTATION PAGE

Form Approved
OMB No. 0704-0188

1. REPORT DATE *(DD-MM-YYYY)*	**2. REPORT TYPE**	**3. DATES COVERED** *(From - To)*
01-09-2006	Final	15 May 2002 – 31 Aug 2006

4. TITLE AND SUBTITLE

Use of Epidermolysis Bullosa Biomarkers in Models of Vesicant Injury

5a. CONTRACT NUMBER

5b. GRANT NUMBER
DAMD17-02-C-0091

5c. PROGRAM ELEMENT NUMBER

6. AUTHOR(S)

Donald R. Gerecke, Ph.D.

E-Mail: gerecke@eohsi.rutgers.edu

5d. PROJECT NUMBER

5e. TASK NUMBER

5f. WORK UNIT NUMBER

7. PERFORMING ORGANIZATION NAME(S) AND ADDRESS(ES)

Rutgers the State University of New Jersey
Piscataway, New Jersey 08854-8010

8. PERFORMING ORGANIZATION REPORT NUMBER

9. SPONSORING / MONITORING AGENCY NAME(S) AND ADDRESS(ES)
U.S. Army Medical Research and Materiel Command
Fort Detrick, Maryland 21702-5012

10. SPONSOR/MONITOR'S ACRONYM(S)

11. SPONSOR/MONITOR'S REPORT NUMBER(S)

12. DISTRIBUTION / AVAILABILITY STATEMENT
Approved for Public Release; Distribution Unlimited

13. SUPPLEMENTARY NOTES

14. ABSTRACT

Executive Summary....see next page

15. SUBJECT TERMS
Epidermolysis Bullosa
Biomarkers Vesicant Injury

16. SECURITY CLASSIFICATION OF:			**17. LIMITATION OF ABSTRACT**	**18. NUMBER OF PAGES**	**19a. NAME OF RESPONSIBLE PERSON**
a. REPORT	**b. ABSTRACT**	**c. THIS PAGE**			USAMRMC
U	U	U	UU	52	**19b. TELEPHONE NUMBER** *(include area code)*

Standard Form 298 (Rev. 8-98)
Prescribed by ANSI Std. Z39.18

EXECUTIVE SUMMARY

This study consisted of an SM time course study for gene expression of protease and extracellular matrix related genes and an evaluation of potential medical countermeasures for SM-induced injury in the mouse ear vesicant model. The specific aim of the time course study was to determine whether MMP and MMP substrate (laminin-332) gene expression levels are altered over time (6, 12, 24, 72, 168 h) in mouse ear skin topically exposed to liquid SM. The specific aim of the compound evaluation study was to determine the effectiveness of topically delivered synthetic MMP inhibitors, Ilomastat, GM1489, MMP-2/MMP-9 Inhibitor I, and MMP-2/MMP-9 Inhibitor II, to protect against SM injury. Protection was quantitatively assessed by measuring MMP and MMP substrate gene expression levels with subsequent correlation to histopathological damage in tissues harvested at 24 h, 72 h and 7 days after SM challenge. Pre-treatment with Ilomastat in conjunction with SM exposure significantly decreased laminin-γ2 expression at 72 h and significantly increased laminin332-α3A expression at 72 h as compared to SM-only (no drug compound pre-treatment). This coincided with a slightly improved Draize Score at 72 h with Ilomastat pre-treatment as compared to the other compounds. Pre-treatment with GM1489 in conjunction with SM exposure significantly decreased MMP-9 expression at 72 h and decreased MMP-2 expression at 7 days as compared to SM-only. Pre-treatment with MMP-2/MMP-9 Inhibitor I in conjunction with SM exposure significantly decreased MMP-2, laminin-γ2, laminin5-α3A, and laminin-β3 expression at 7 days and increased laminin-β3 and laminin5-α3A expression at 72 h as compared to SM-only. Pre-treatment with MMP-2/MMP-9 Inhibitor II in conjunction with SM exposure significantly increased laminin 332-α3A expression at 24 h as compared to SM-only. Gene expression profiles support the identification of specific targets for therapeutic countermeasures against SM-induced skin injury and provide additional biochemical markers for understanding SM toxicity. *In vitro* mouse keratinocyte studies also show promise as a potential future alternative vesicant model.

TABLE OF CONTENTS

INTRODUCTION

Sulfur mustard (bis(2-chloroethyl)sulfide, SM, HD) is a chemical warfare agent that penetrates the skin rapidly and causes extensive blistering after a latent period of several hours [1]. Currently, there are few established prophylactic or therapeutic countermeasures against SM-induced skin injury and there is great interest in discovering more. Although the specific pathogenic and molecular mechanisms responsible for SM-induced skin injury remain unclear, it has been established that cutaneous exposure to SM results in inflammation, epithelial tissue damage, and damage to the anchoring complex of the dermal-epidermal junction (DEJ), culminating in the formation of subepidermal blisters [1]. Laminin-332 (formerly called laminin-5)[2] is a glycoprotein that is crucial to keratinocyte adhesion. It is assembled as part of an ultrastructural feature of the skin, the "anchoring complex" which is composed of a continuum of molecules that originates within the epithelial cell, extends into the underlying ECM, and functions to reinforce cell-matrix attachment[3]. This attachment helps maintain the integrity of skin against externally applied force. There are many structural proteins involved in these interactions, including keratins, bullous pemphigoid antigens (BPAG), laminin isoforms, and type VII collagen [4;5]. If the attachment of any of these proteins is disrupted, the skin, which becomes fragile, can pull loose from the underlying dermis. This is exemplified by epidermolysis bullosa (EB), a group of skin diseases characterized by fragility and easy blistering of the skin in response to mechanical trauma. The clinical severity and extent of tissue involvement in EB are highly variable, as reflected in the extensive and primarily descriptive nomenclature developed for these conditions in the past [6]. Clinical, morphological, and ultrastructural observations have been used to classify inherited EB into three major categories on the basis of the level of blister formation within the skin: the simplex (EBS), junctional (JEB), and dystrophic (DEB) forms. There is a similarity between SM-induced skin injury and EB [7]. It was reported that 4 to 6 hours after accidental exposure to sulfur mustard, the victim had skin pathology that involved targeting of epidermal basal cells, disabling of hemidesmosomes, and recruitment of inflammatory cells similar to that seen in EB syndrome[7]. Another study demonstrated EB-like separation of the epidermis and dermis in mouse ears treated with SM [8]. This separation caused by SM exposure is most similar to the junctional epidermolysis bullosa which is an autosomal recessive skin blistering disease with both lethal and nonlethal forms[9]. As with

SM exposure, in JEB, the skin blistering occurs at the lamina lucida and is involved with the hemidesmosomal proteins that attach basal keratinocytes to the basement membrane zone (BMZ) [10]. One of the major proteins of the lamina lucida that anchor the keratinocytes is laminin-332 which is made up of three individual polypeptides that are separate gene products. These genes have been named LAMA3[11]; LAMB3[3]; and LAMC2[12] and their molecular weights are α3 of 200 kDa; β3 of 145 kDa; and γ2 of 155 kDa [13]. There has been extensive mutation detection analysis in JEB patients and mutations in any of these three separate polypeptide genes have been shown to cause JEB[14]. Ultrastructural evidence of SM-induced basal cell BMZ damage has been documented for both laminin-332 and bullous pemphigoid 180 [7;8;15]. These morphological similarities between EB- and SM-induced skin injuries are the rationale for studying the laminin-332 polypeptide chains.

Proteases are elevated in cutaneous inflammatory responses[16] and are known to play key roles in the disruption of connective tissue proteins and other basement membrane proteins[17]. One particular class of proteases is the matrix metalloproteinases (MMPs) which are zinc- and calcium-dependent endopeptidases that function in the turnover of extracellular matrix components. They are a family of protein enzymes, and in vertebrates, there are at least sixteen secreted MMPs and six membrane-type MMPs[18]. The skin can produce a number of MMPs, including, MMP-1, MMP-2, MMP-3, MMP-7, MMP-9, MMP-10, MMP-12, and MMP-13, and many of these are upregulated in response to injury. It is suggested that proteases released following cutaneous SM exposure are involved in damage to key basement membrane zone (BMZ) and extracellular matrix (ECM) components, such as laminin[19]. Some of the same proteases that are released or induced because of inflammation, tissue damage, or cell death may be involved in both SM-induced and EB initiated inflammation because their morphological outcomes are so similar. Skin fibroblasts from patients with EDEB have been reported to have an abnormally high level of collagenase and/or stromelysin[20;21]. The simplex form of EB has been shown to express high levels of gelatinases (MMP-2 and MMP-9). Proteases also are implicated in other subepidermal blistering diseases, such as bullous pemphigoid, dermatitis herpetiformis, and pemphigus vulgaris[22]. Because proteases are likely to be involved in the pathophysiology of SM-induced blistering, the effectiveness of protease inhibitors as therapeutic agents against SM

skin damage should be investigated. In fact, several reports showed some success in the use of protease inhibitors both *in vitro* in cell culture[23] and *in vivo* in a mouse model[24;25].

Mouse keratinocytes in culture have the potential for use in compound evaluation studies, but have been extremely difficult to grow as primary cultures and their use as subcultures have been nearly impossible. Recently two papers reported a new method for growing newborn mouse keratinocytes for up to 19 passages[26;27]. This would allow for the development of an *in vitro* method of testing EB biomarkers and relate them to SM-induced biomarkers. The same BEB and MMP biomarkers can be examined in cell culture and compared to the levels found in live animal skin. This would greatly reduce the number of live animals required for these studies.

As a means to study the similarities between EB and SM-treated skin, evaluate MMP inhibitors, and test mouse keratinocytes in culture, we propose the following statement of work:

STATEMENT OF WORK

1. *Animal Exposure and Skin Specimen Collection*: Using the mouse ear vesicant model (MEVM), 8-mm ear skin punch biopsy specimens in addition to the remaining tissue from punched excised ear skin, will be taken and utilized for biochemical and molecular studies. Tissue collected at specified times (i.e., 6, 12, 24, 72, hr) after exposure to cutaneous sulfur mustard (SM).
2. *Molecular Studies:* Biomarkers of epidermolysis bullosa (BEB), laminin alpha 3, laminin beta 3 and laminin gamma 2, and the matrix metalloproteinases (MMP) 2 and 9, will be identified and quantified in SM-exposed or unexposed mouse skin specimens using RT-PCR.
3. *Animal Exposure and Skin Specimen Collection*: Using the MEVM, examine up to six compounds delivered topically prior to SM challenge. At specified times (i.e., 24, 72 hr) following SM challenge, 8-mm ear skin punch biopsy specimens, in addition to the remaining tissue from punched excised ear skin, will be taken and utilized for biochemical, molecular, and histopathological studies.
4. *Molecular Studies*: Increased BEB and MMP mRNA levels from SM-exposed mouse skin specimens identified and quantified in Section 2. will be examined using RT-PCR.
5. *Histopathology*: Hematoxylin and Eosin stained tissue specimens will be examined by light microscopy only in those animals whose ear weight was significantly reduced by a candidate inhibitor compound.

6. *Molecular Studies*: BEBs and MMPs will be identified and quantified in mouse keratinocyte cell culture specimens using RT-PCR.

The total time necessary to perform and evaluate these studies is estimated to be 36 months. The time-phased breakdown is as follows:

1, 2	**Animal exposure to SM and molecular characterization of BEBs and MMPs in the mouse ear vesicant model**	**10 months**
3, 4, 5	**Examine up to six compounds in the mouse ear vesicant model, molecular characterization of BEBs and MMPs, and histopathology**	**18 months**
6	**Molecular characterization of BEBs and MMPs in mouse keratinocyte cell culture specimens**	**6 months**

MATERIALS AND METHODS

SM (SM) and Compound Exposure

Male CD1 mice (Charles River Laboratories, Portage, MI; N = 20 per treatment) were anesthetized with ketamine and xylazine and exposed to SM and/or compound as previously described (7, 8). Briefly, five μL of 97.5 mM SM (0.08 mg) in CH_2Cl_2 (methylene chloride) was applied to the inner medial surface of the right ear. The left ear served as a control and received only the vehicle CH_2Cl_2. For the time course study, animals were euthanized at 6, 12, 24, and 72 h post-exposure and dermal punch specimens (8 mm in diameter) were taken from the center of both the SM-exposed and control ears. The ear punch was weighed to measure edema and then either snap-frozen in liquid nitrogen and stored at -70ºC or fixed in neutral-buffered formalin for approximately 24 h at room temperature. After approximately 24 h the formalin-fixed tissues were rinsed in phosphate buffer saline (PBS) and stored at 4°C. The relative skin weight (RSW) between SM-treated and control groups was calculated [(weight of right ear - weight of left ear) / weight of left ear x 100] and statistical analyses were conducted using a one-way ANOVA (Statistica, StatSoft, Tulsa, OK). Statistical significance was defined as $P \leq 0.05$.

For the compound evaluation study, animals were divided into three treatment groups (Table 1). The compounds evaluated were Ilomastat, GM1489, MMP-2/MMP-9 Inhibitor I, and MMP-2/MMP-9 Inhibitor II (Calbiochem, SanDiego, CA). Group 1 received 5 μL of 97.5 mM SM (0.08 mg) in CH_2Cl_2 (methylene chloride) applied to the inner medial surface of the right ear and 5 μL of CH_2Cl_2 only applied to the left ear (left ear served as a control). Group 2 received 20 μL of 25 mM compound in ethanol applied to the right ear and 20 μL of ethanol only applied to the left ear (left ear served as a control). Group 2 was not exposed to SM. Group 3 received 20 μL of 25 mM compound in ethanol applied to the right ear and 20 μL of ethanol only applied to the left ear followed 15 minutes later with 5 μL SM applied to the right ear and 5 μL CH_2Cl_2-only applied to the left ear. At specified times (24 h, 72 h, and 7 days post-exposure) animals were euthanized and dermal punch specimens (8 mm in diameter) were taken from the center of both the right and left ears. The ear punch was weighed to measure edema and then either snap-frozen in liquid nitrogen and stored at -70ºC

or fixed in neutral-buffered formalin for approximately 24 h at room temperature. The formalin-fixed tissues were rinsed in PBS and stored at 4°C.

Table 1. Treatment Groups for Compound Evaluation Study

Treatment Group	Right Ear	Left Ear
1	SM	CH_2Cl_2
2	Compound	Ethanol
3	Compound followed by SM	Ethanol followed by CH_2Cl_2

RNA Isolation and Reverse Transcription

Total RNA was isolated using TRIzol according to the instructions of the manufacturer (Invitrogen, Carlsbad, CA) with the addition of PhaseLock Gel (Brinkman Eppendorf, Westbury, NY) during centrifugation to allow separation of the phenol-chloroform phase from the aqueous phase. The RNA pellet was dissolved in RNA Storage Solution (Ambion, Austin, TX). RNA was quantitated spectrophotometrically based on an absorbance at 260 nm of one equal to an RNA concentration of 40 μg/mL. Total RNA (1 μg) was reverse-transcribed into cDNA using SuperScript™ III First-Strand Synthesis System for RT-PCR (Invitrogen, Gaithersburg, MD). A minus reverse transcriptase reaction was included as a control.

Real-Time Polymerase Chain Reaction (PCR)

Primer and probe sets for MMP-2, MMP-9, laminin-γ2, laminin5-α3A, and laminin-β3 were designed using the Assay-by-Design service of Applied Biosystems (Applied Biosystems, Foster City, CA) (Tables 2 and 3). Real-time PCR was performed an ABI Prism® 7900 HT Fast Real-Time-PCR Sequence Detection System. Hypoxanthine guanine phosphoribosyl transferase (HPRT) expression levels were used as an endogenous control. Three μL of cDNA was added to a 50 μL reaction. Assays were performed in duplicate and averaged. No template controls were negative for amplification. Threshold cycle (C*t*), which correlates inversely with the target mRNA levels, was measured as the cycle number at which the reporter fluorescent emission increased above a threshold level.

The comparative C*t* method was used to determine relative mRNA expression levels for each of the test genes in the ear tissue samples. C*t* values for gene amplification were normalized by subtracting the C*t* values for HPRT using the equation: $Ct_{(gene)} - Ct_{(HPRT)} = \Delta Ct$. The ΔCt values for the control skin were subtracted from the SM-exposed skin ΔCt values to calculate the fold change in gene expression: $\Delta Ct_{(exposed)} - \Delta Ct_{(control)} = \Delta\Delta Ct$. Fold increases in gene expression were calculated by the following equation according to ABI User Bulletin #2: $2^{-\Delta\Delta Ct}$ = fold change in expression. Data is expressed as fold change.

Table 2. Gene Accession Numbers

Gene Name	Accession Number
Matrix metalloproteinase 2 (MMP-2)	NM_008610
Matrix metalloproteinase 9 (MMP-9)	Z27231
Laminin-γ2	U43327
Laminin-β3	NM_008484
Laminin-5α3A	X84013
Hypoxanthine guanine phosphoribosyl transferase (HPRT)	NM_013556

Table 3. Assay by Design Primer/Probe Sets

Forward Primer Name	**Forward Primer Sequence**
MMP2-529F	GCTGACATCATGATCAACTTTGGA
MMP9-997F	ACCAGGATAAACTGTATGGCTTCTG
Lamin-gam2-2306F	GCTCAGGAGGCTACAAGAAAGG
Lamin-5a3A-786F	AACAGATCCGGCACATGGA
Lamin-b3-2128F	GCAATTTGAGAAGCTAAGCAGTGA
MHPRT-485F	CAGTACAGCCCCAAAATGGTTAA
Reverse Primer Name	**Reverse Primer Sequence**
MMP2-529R	GCCATCAAACGGGTATCCAT
MMP9-997R	ACAGCTCTCCTGCCGAGTTG
Lamin-gam2-2306R	TGCTTCATTGCGTTAGCTGACT
Lamin-5a3A-786R	CCATGACTTGAGGTGGCAGAA
Lamin-b3-2128R	AGGACTGCTCATAAGCCATGGT
MHPRT-485R	AACACTTCGAGAGGTCCTTTTCAC
Probe Name	**Probe Sequence**
MMP2-529M1	CGCTGGGAGCATGG
MMP9-997M1	TACCCGAGTGGACGCG
Lamin-gam2-2306M2	AGCGTGGCTGTCTG
Lamin-5a3A-786M1	CCTGAGGAACCAGCTG
Lamin-b3-2128M1	CCTTCAGGAGCCTTC
MHPRT-485M2	CAGCAAGCTTGCAACC

RESULTS

Time Course of SM-Induced Skin Inflammation

Skin edema was determined at 6, 12, 24, and 72 h post-exposure and expressed as RSW (Table 4). A significant increase ($P \leq 0.05$) in RSW was observed in SM-treated skin over the observed time period. When compared to control skin weight, the mean SM-treated skin weight at each time period was significantly higher ($P <\leq 0.05$) than the respective controls. Edema was apparent within 12-24 h (Figure 1). At higher magnifications differences between the untreated (A and B) and treated samples were noted at 6 h post-treatment (Figure 2). By 12 h, an infiltration of inflammatory cells was observed in treated versus untreated samples (Figure 3). Damage to the epithelia increased with time and necrosis of basal cells and the appearance of subepidermal blisters was observed at 24 h (Figure 4) and 72 h (Figure 5) post-treatment. The 24 h and 72 h post-treatment samples also exhibited contralateral ear damage, secondary to the primary event (Figures 4 and 5). This was defined by the appearance of basal cell necrosis and subepidermal blisters on the untreated side of the ears (the outer ear).

Table 4. Relative Skin Weight for the Time Course Study

Time Post Exposure	Control Skin Weight (g)	SM-Treated Skin Weight (g)	RSW
6 h	0.0148	0.0190	29.1
12 h	0.0145	0.0340	134.9
24 h	0.0139	0.0372	168.5
72 h	0.0150	0.0458	207.1

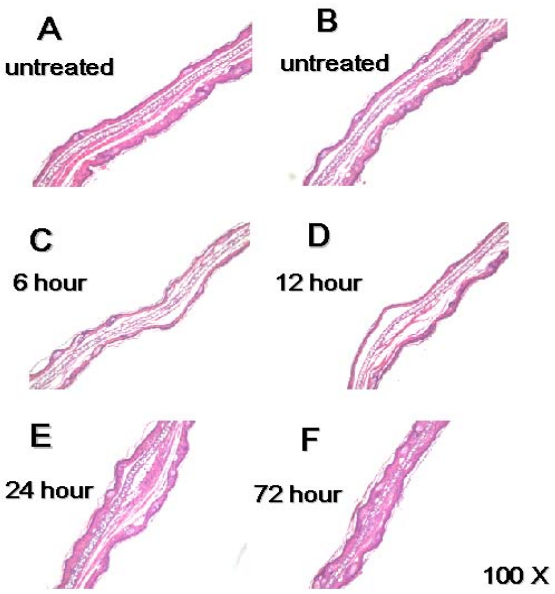

Figure 1. H & E staining from untreated (A and B) and SM-treated (C-F) mouse ear biopsy samples collected 6 (C), 12 (D), 24 (E), or 72 (F) h after SM exposure. The outer ear is toward the right and the inner ear toward the left. Magnification was 100X.

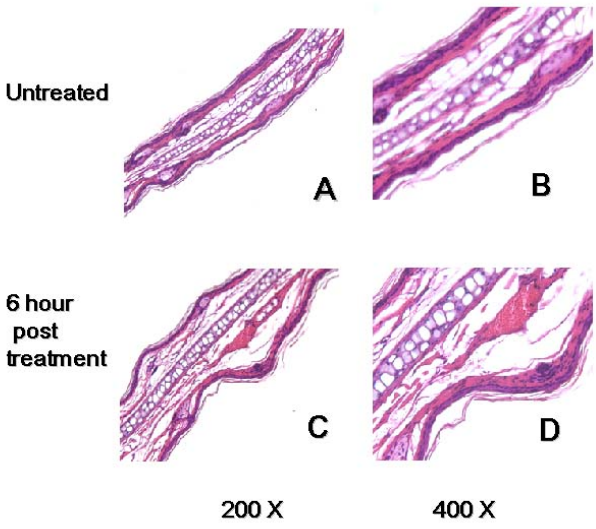

Figure 2. H & E staining from untreated (A and B) and 6 h post-SM-treated (C and D) mouse ear biopsy samples. Inner ear (treated) is to left and outer ear to right. Magnification either 200 X or 400X.

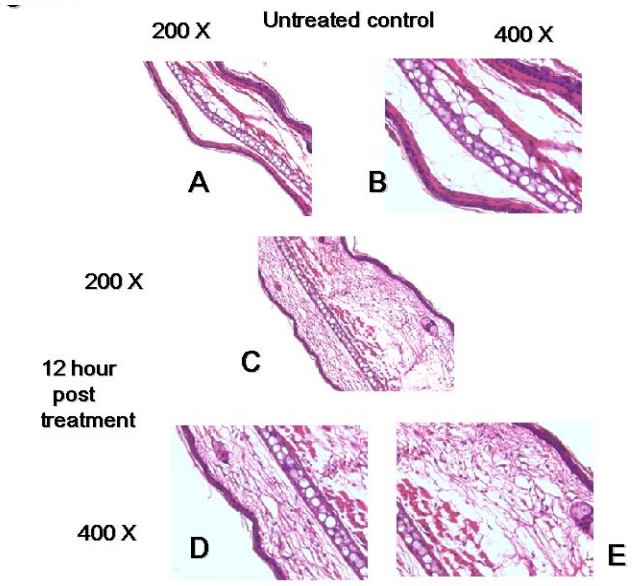

Figure 3. H & E staining from untreated (A and B) and 12 h post-SM-treated (C-E) mouse ear biopsy samples. Inner ear (treated) is to left and outer ear to right. Magnification either 200 X or 400X.

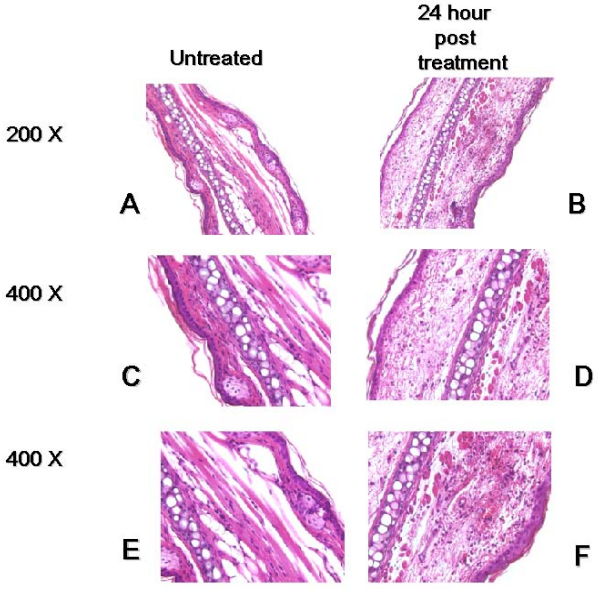

Figure 4. H & E staining from untreated (A, C, E) and 24 h post-SM-treated (B, D, F) mouse ear biopsy samples. Inner ear (treated) is to left and outer ear to right. Magnification either 200X or 400X.

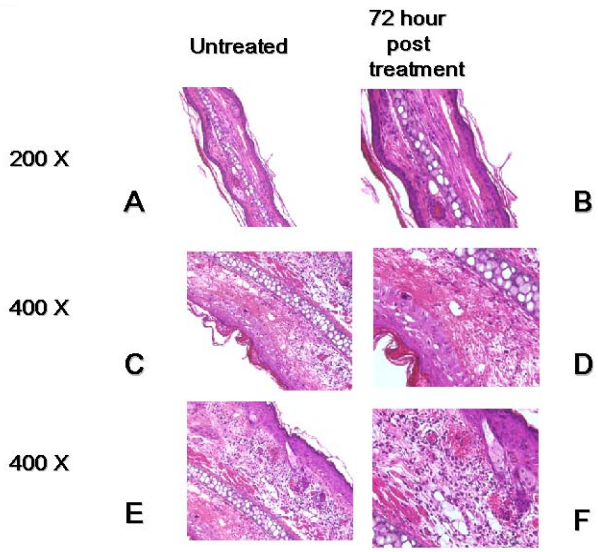

Figure 5. H & E staining from untreated (A, C, E) and 72 h post-SM-treated (B, D, F) mouse ear biopsy samples. Inner ear (treated) is to left and outer ear to right. Magnification either 200X or 400X.

Compound Evaluation Study

Skin edema was determined at 24 h, 72 h, and 7 days post-exposure and expressed as RSW (Table 5). Daily variation in ear tissue weights is normal when comparing weight changes between the SM-only and compound + SM treated groups. Because of these normal variations, statistics were not performed to determine if there was a significant difference in RSW between the SM-treated groups and the compound plus SM-treated groups at each time period. If a dramatic decrease had been observed, then further statistical analyses would be warranted. In the groups progressing to Day 7, the ear tissue became necrotic, and in many instances it was difficult to obtain a tissue specimen. Therefore, ear tissue weight at this time point is uninformative.

Table 5. Relative Skin Weight for Compound Evaluation Study

Compound	Time Post Exposure	RSW Compound + SM(g)	RSW SM-only(g)	RSW Compound only (g)
Ilomastat	24 h	146.2	138.4	0.1
	72 h	186.6	231.8	-2.7
	7 days	242.7	200.8	-3.0
GM1489	24 h	155.9	168.0	-0.7
	72 h	185.7	175.9	-1.8
	7 days	104.5	115.1	-1.4
MMP-2/ MMP-9 Inhibitor I	24 h	129.1	114.3	0
	72 h	154.1	124.6	-0.7
	7 days	173.5	160.4	-5.5
MMP-2/ MMP-9 Inhibitor II	24 h	148.0	154.5	0.9
	72 h	179.4	195.1	1.8
	7 days	161.0	146.4	0.5

To grade the extent of ear tissue damage, a modified Draize ear tissue scoring system was also conducted randomly at 24 h, 72 h, and 7 days. Scores range from 0 = unchanged from control tissue; 1 = edema and/or erythema; 2 = focal areas of necrosis, but tissue still pliable; 3 = less than 50% of tissue is necrotic, tissue firm and dry, and 4 = more than 50% of tissue is necrotic, tissue firm and dry. Scores at 24 h are all rated as "1", so no distinction between treatment groups can be made (Table 4). Scores at 7 days are reflective of mostly necrotic tissue (Table 6). There was a slight decrease in Draize scores when comparing SM treatment only to compound + SM treatment (Table 6).

Table 6. Draize Scores for Compound Evaluation Study

Compound	Time Post Exposure	Average Draize Scores Compound + SM	Average Draize Scores SM only
Ilomastat	24 h	1.0	1.0
	72 h	2.15	2.55
	7 days	3.9	3.95
GM1489	24 h	1.0	1.0
	72 h	2.2	2.6
	7 days	3.05	3.45
MMP-2/ MMP-9 Inhibitor I	24 h	1.0	1.0
	72 h	2.8	2.45
	7 days	3.7	3.8
MMP-2/ MMP-9 Inhibitor II	24 h	1.0	1.0
	72 h	2.5	2.45
	7 days	3.65	3.8

SM-Induced Gene Expression

PCR primer/probe sets were evaluated in real-time PCR using normal mouse ear tissue as the source of RNA for cDNA synthesis (Table 7). Each primer/probe set amplified its respective gene. The PCR primer/probes sets were then used to evaluate the gene expression levels of the genes in each of the samples from both the time-course study and the compound evaluation study.

Table 7. Evaluation of Primer/Probe Sets by Real-Time PCR with Normal Mouse Ear Tissue

Sample ID	Gene	C_T1	C_T2	C_T AVG
1-101-00-1	HPRT	25.39	25.43	25.69
1-101-00-2	HPRT	25.93	25.80	
1-102-00-1	HPRT	25.73	25.85	
1-101-00-1	MMP-2	19.04	19.11	19.21
1-101-00-2	MMP-2	19.18	19.21	
1-102-00-1	MMP-2	19.35	19.35	
1-101-00-1	MMP-9	25.33	NP	25.46
1-101-00-2	MMP-9	25.26	NP	
1-102-00-1	MMP-9	25.80	NP	
1-101-00-1	Laminin-γ2	27.04	NP	27.38
1-101-00-2	Laminin-γ2	27.59	NP	
1-102-00-1	Laminin-γ2	27.51	NP	
1-101-00-1	Laminin5-α3A	22.48	NP	22.60
1-101-00-2	Laminin5-α3A	22.75	NP	
1-102-00-1	Laminin5-α3A	22.56	NP	
1-101-00-1	Laminin-β3	23.16	NP	23.33
1-101-00-2	Laminin-β3	23.48	NP	
1-102-00-1	Laminin-β3	23.34	NP	

NP = Not Performed

For the time course study, gene expression levels were determined using real-time PCR in mouse ear tissue samples at 6, 12, 24, and 72 h post-exposure to SM. Data are presented graphically with geometric means and 95% confidence intervals (Figures 6 – 10) and in tabular form (Table 8). MMP-2 expression levels decreased from 6 to 24 h post-exposure and remained decreased at 72 h post-exposure (Figure 6). MMP-9 expression levels increased over the observed time period approximately 6-fold (Figure 7). Laminin-γ2 expression levels initially decreased at 6 and 12 h post-exposure followed by an increase at 24 h and 72 h post-exposure to approximately 6-fold (Figure 8). Laminin5-α3A expression levels were decreased at 6, 12, and 24 h post-exposure followed by an increase at 72 h post-

exposure (Figure 9). Laminin-β3 expression levels initially decreased at 6, 12, and 24 h post-exposure followed by a slight increase at 72 h (Figure 10).

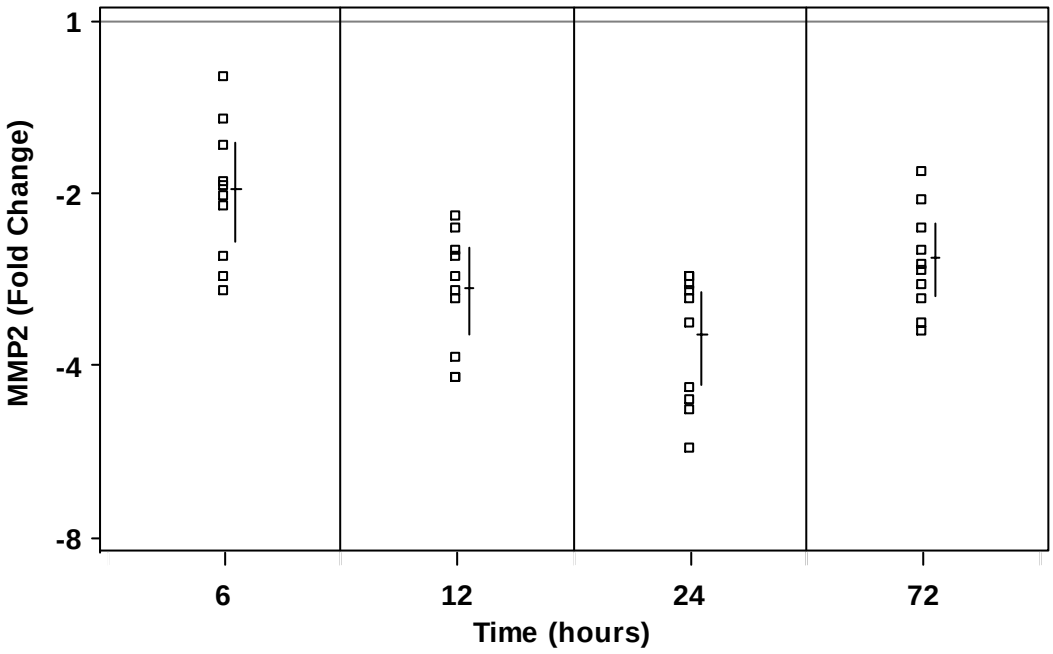

Figure 6. **Fold Change in MMP-2 mRNA in Mouse Skin.** Relative MMP-2 mRNA expression levels in mouse ear skin following a 0.08 mg SM cutaneous exposure compared to vehicle control at 6, 12, 24, and 72 h post-exposure. Individual data points are indicated by squares. The horizontal dashes represent the geometric mean and the vertical lines represent the 95% confidence intervals.

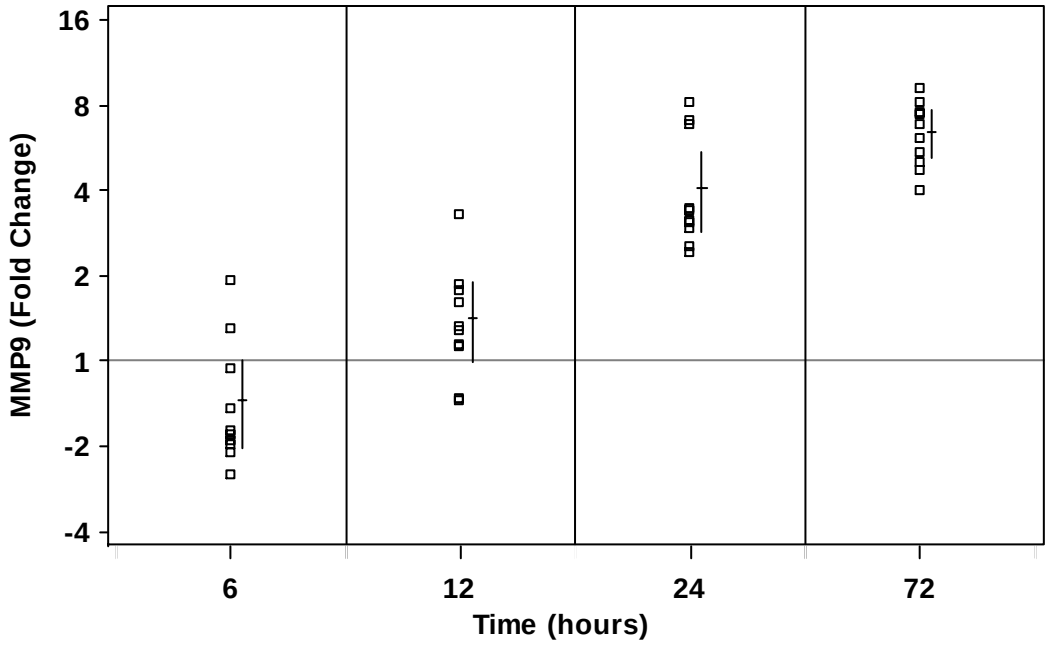

Figure 7. Fold Change in MMP-9 mRNA in Mouse Skin. Relative MMP-9 mRNA expression levels in mouse ear skin following a 0.08 mg SM cutaneous exposure compared to vehicle control at 6, 12, 24, and 72 h post-exposure. Individual data points are indicated by squares. The horizontal dashes represent the geometric mean and the vertical lines represent the 95% confidence intervals.

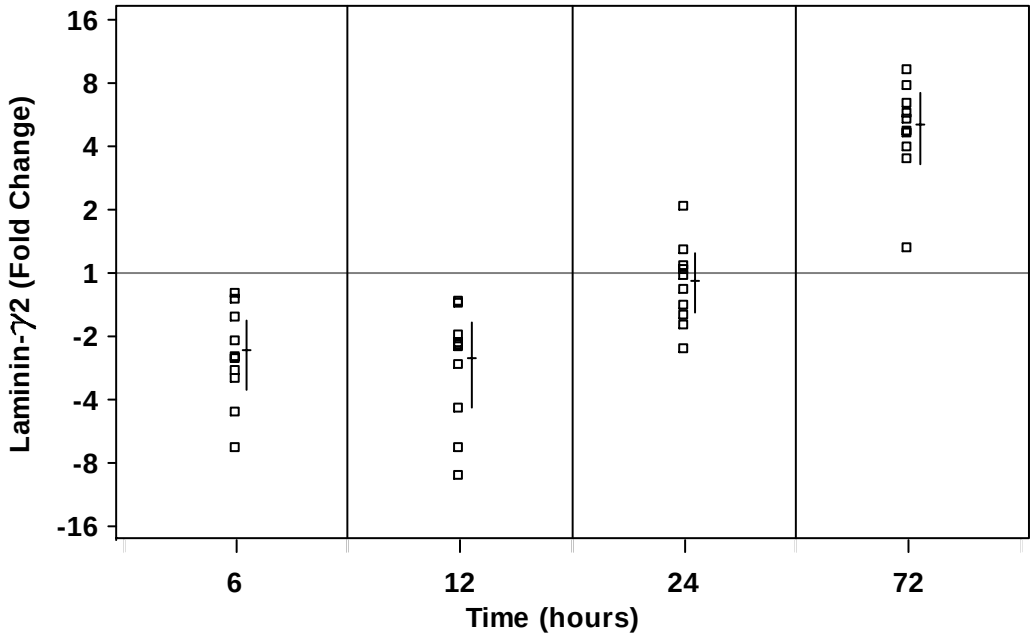

Figure 8. Fold Change in Laminin-γ2 mRNA in Mouse Skin. Relative laminin-γ2 mRNA expression levels in mouse ear skin following a 0.08 mg SM cutaneous exposure compared to vehicle control at 6, 12, 24, and 72 h post-exposure. Individual data points are indicated by squares. The horizontal dashes represent the geometric mean and the vertical lines represent the 95% confidence intervals.

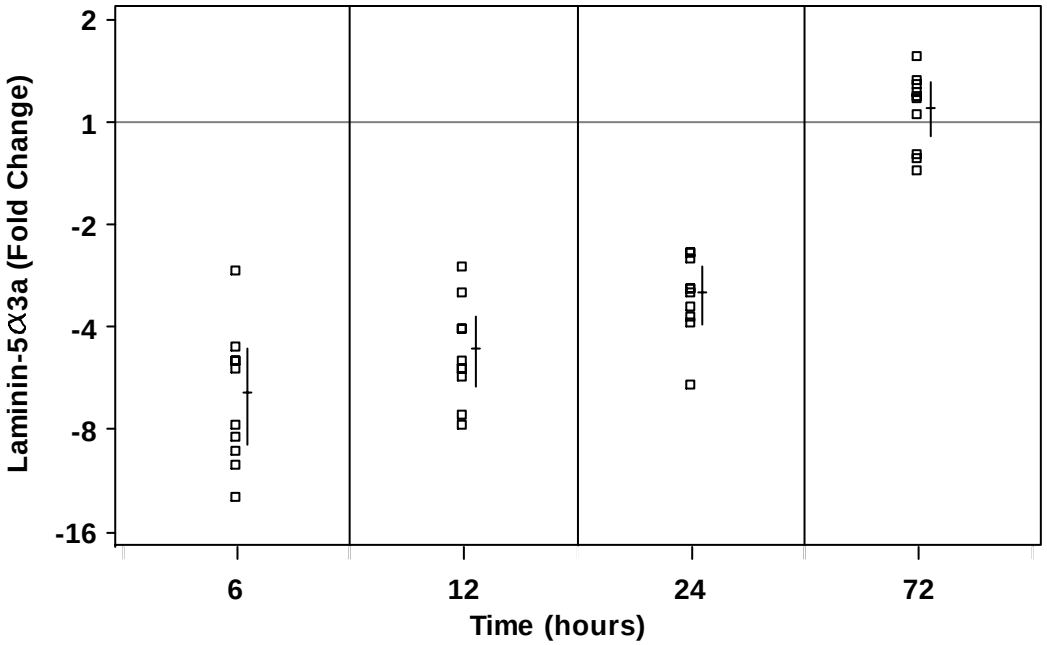

Figure 9. Fold Change in Laminin5-α3A mRNA in Mouse Skin. Relative laminin5-α3A mRNA expression levels in mouse ear skin following a 0.08 mg SM cutaneous exposure compared to vehicle control at 6, 12, 24, and 72 h post-exposure. Individual data points are indicated by squares. The horizontal dashes represent the geometric mean and the vertical lines represent the 95% confidence intervals.

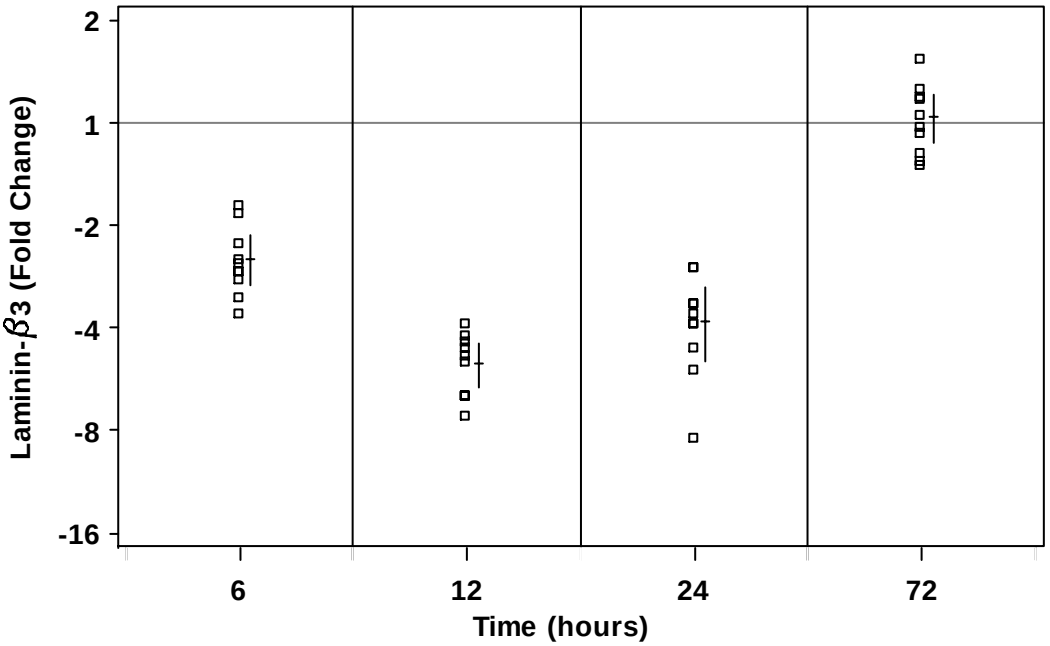

Figure 10. Fold Change in Laminin-β3 mRNA in Mouse Skin. Relative laminin-β3 mRNA expression levels in mouse ear skin following a 0.08 mg SM cutaneous exposure compared to vehicle control at 6, 12, 24, and 72 h post-exposure. Individual data points are indicated by squares. The horizontal dashes represent the geometric mean and the vertical lines represent the 95% confidence intervals.

Table 8. Relative mRNA expression levels of MMP-2, MMP-9, laminin-γ2, laminin-5α3A, and laminin-β3 in mouse ear skin following a 0.08 mg SM cutaneous exposure compared to vehicle control at 6, 12, 24, and 72 h post-exposure.

Target Genes	Time (Hours)	SM Only		
		Fold Change (Geometric Mean)	95% Confidence Interval	
			Lower	Upper
MMP-2	6	-2.00	-2.44	-1.64
MMP-2	12	-2.94	-3.57	-2.50
MMP-2	24	-3.57	-4.35	-2.94
MMP-2	72	-2.63	-3.03	-2.27
MMP-9	6	-1.43	-2.04	1.00
MMP-9	12	1.37	-1.01	1.89
MMP-9	24	3.94	2.84	5.46
MMP-9	72	6.33	5.24	7.65
Laminin-γ2	6	-2.50	-3.57	-1.69
Laminin-γ2	12	-2.78	-4.35	-1.75
Laminin-γ2	24	-1.12	-1.54	1.23
Laminin-γ2	72	4.83	3.29	7.10
Laminin-5α3A	6	-6.25	-9.09	-4.55
Laminin-5α3A	12	-4.76	-5.88	-3.70
Laminin-5α3A	24	-3.23	-3.85	-2.63
Laminin-5α3A	72	1.09	-1.10	1.31
Laminin-β3	6	-2.50	-2.94	-2.13
Laminin -β3	12	-5.26	-5.88	-4.35
Laminin -β3	24	-3.85	-5.00	-3.03
Laminin -β3	72	1.03	-1.15	1.22

For the compound evaluation studies, gene expression analysis were performed for Ilomastat (Figures 11-15, Table 9), GM1489 (Figures 16-20, Table 10), MMP-2/MMP-9 Inhibitor I (Figures 21-25, Table 11), and MMP-2/MMP-9 Inhibitor II (Figures 26-30, Table 12). Data are presented graphically with geometric means and 95% confidence intervals (Figures 11-30) and in tabular form (Tables 9-12). Pre-treatment with Ilomastat in conjunction with SM exposure significantly decreased laminin-γ2 expression at 72 h and significantly increased laminin5-α3A expression at 72 h as compared to SM-only (no drug compound pre-treatment) (Tables 9 and 13). Pre-treatment with GM1489 in conjunction with SM exposure significantly decreased MMP-9 expression at 72 h and decreased MMP-2 expression at 7 days as compared to SM-only (Tables 10 and 13). Pre-treatment with MMP-2/MMP-9 Inhibitor I in conjunction with SM exposure significantly decreased MMP-2, laminin-γ2, laminin5-α3A, and laminin-β3 expression at 7 days and increased laminin-β3

and laminin5-α3A expression at 72 h as compared to SM-only (Tables 11 and 13). Pre-treatment with MMP-2/MMP-9 Inhibitor II in conjunction with SM exposure significantly increased laminin5-α3A expression at 24 h as compared to SM-only (Tables 12 and 13).

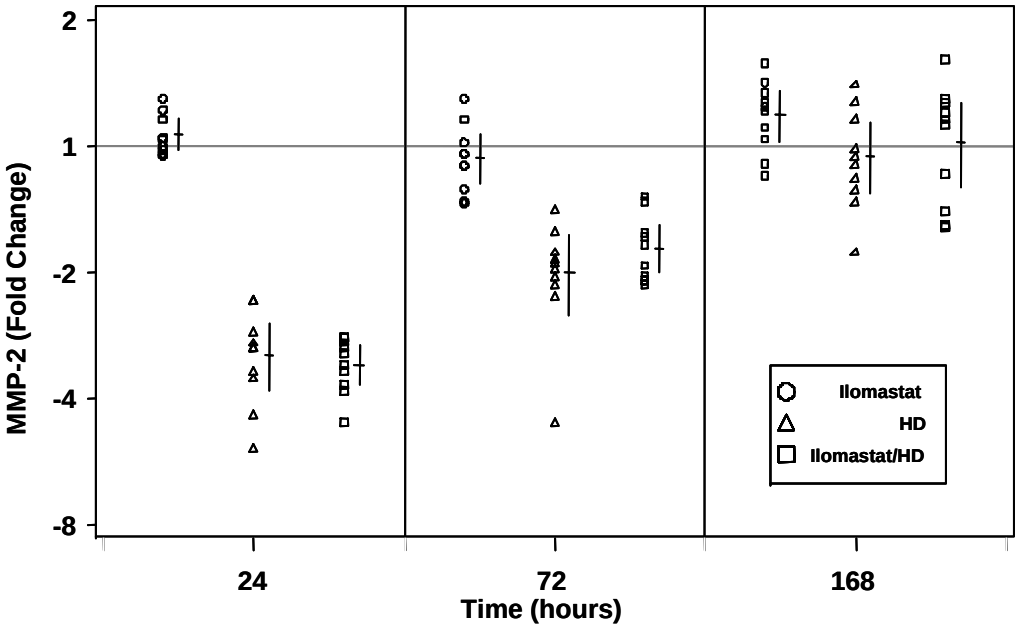

Figure 11. Effect of Ilomastat on MMP-2 mRNA Levels. Fold change in MMP-2 mRNA levels in mouse ear skin pretreated with Ilomastat only (circles), SM-exposed only (triangles), and pretreated with Ilomastat and then SM-exposed (squares) at 24 h, 72 h, and 168 h post-exposure. Individual data points are indicated by the shapes. The horizontal dashes represent the geometric mean and the vertical lines represent the 95% confidence intervals.

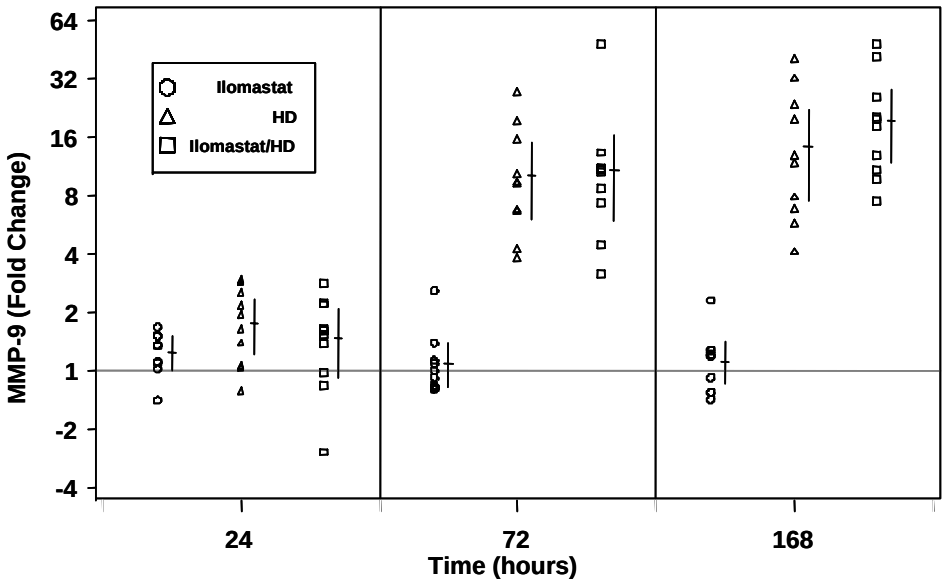

Figure 12. Effect of Ilomastat on MMP-9 mRNA Levels. Fold change in MMP-9 mRNA levels in mouse ear skin pretreated with Ilomastat only (circles), SM-exposed only (triangles), and pretreated with Ilomastat and then SM-exposed (squares) at 24 h, 72 h, and 168 h post-exposure. Individual data points are indicated by the shapes. The horizontal dashes represent the geometric mean and the vertical lines represent the 95% confidence intervals.

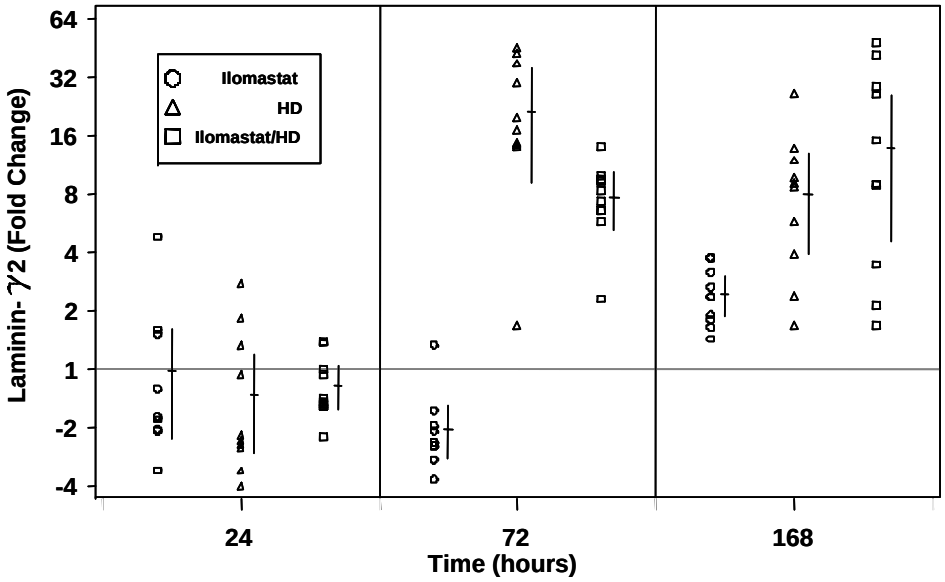

Figure 13. Effect of Ilomastat on Laminin-γ2 mRNA Levels. Fold change in laminin-γ2 mRNA levels in mouse ear skin pretreated with Ilomastat only (circles), SM-exposed only (triangles), and pretreated with Ilomastat and then SM-exposed (squares) at 24 h, 72 h, and 168 h post-exposure. Individual data points are indicated by the shapes. The horizontal dashes represent the geometric mean and the vertical lines represent the 95% confidence intervals.

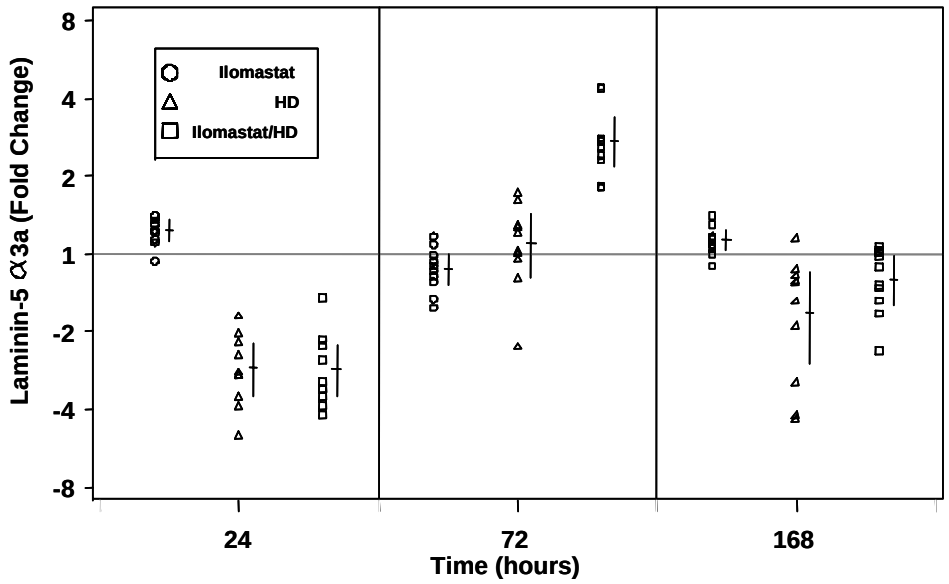

Figure 14. Effect of Ilomastat on Laminin-5α3A mRNA Levels. Fold change in laminin-5α3A mRNA levels in mouse ear skin pretreated with Ilomastat only (circles), SM-exposed only (triangles), and pretreated with Ilomastat and then SM-exposed (squares) at 24 h, 72 h, and 168 h post-exposure. Individual data points are indicated by the shapes. The horizontal dashes represent the geometric mean and the vertical lines represent the 95% confidence intervals.

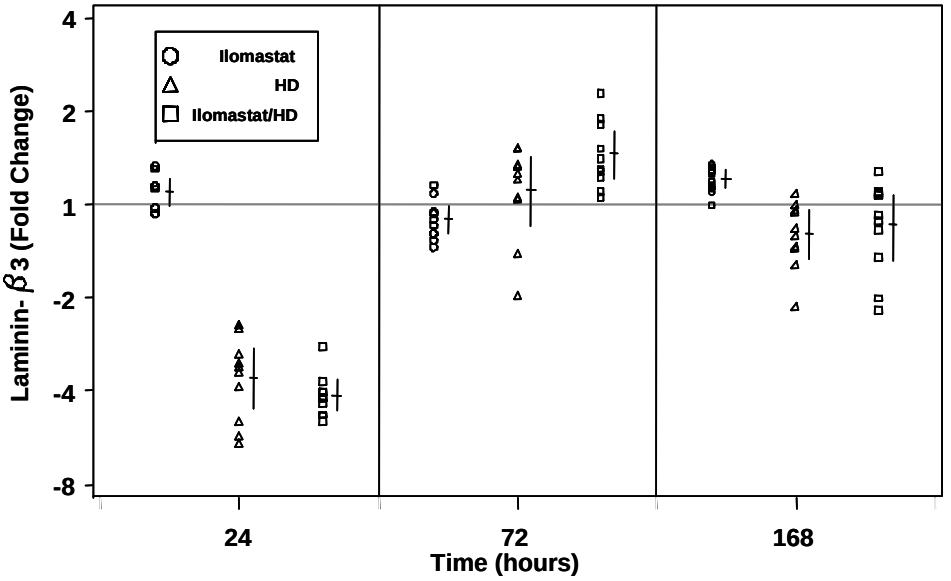

Figure 15. Effect of Ilomastat on Laminin-β3 mRNA Levels. Fold change in laminin-β3 mRNA levels in mouse ear skin pretreated with Ilomastat only (circles), SM-exposed only (triangles), and pretreated with Ilomastat and then SM-exposed (squares) at 24 h, 72 h, and 168 h post-exposure. Individual data points are indicated by the shapes. The horizontal dashes represent the geometric mean and the vertical lines represent the 95% confidence intervals.

Table 9. Relative mRNA expression levels of MMP-2, MMP-9, laminin-γ2, laminin-5α3A, and laminin-β3 in mouse ear skin pretreated with Ilomastat only, SM-exposed only, and pretreated with Ilomastat and then SM-exposed at 24 h, 72 h, and 168 h post-exposure. Shaded values indicate significant difference between SM only and Ilomastat + SSM based on Tukey's multiple comparisons test performed at an overall 0.05 significance level.

Target Genes	Time (Hours)	Ilomastat Only			SM Only			Ilomastat + SM		
		Fold Change (Geometric Mean)	95% Confidence Interval		Fold Change (Geometric Mean)	95% Confidence Interval		Fold Change (Geometric Mean)	95% Confidence Interval	
			Lower	Upper		Lower	Upper		Lower	Upper
MMP-2	24	1.07	-1.02	1.16	-3.23	-3.85	-2.63	-3.33	-3.70	-3.03
MMP-2	72	-1.08	-1.22	1.06	-2.04	-2.56	-1.64	-1.75	-2.00	-1.56
MMP-2	168	1.18	1.02	1.35	-1.08	-1.30	1.14	1.01	-1.25	1.27
MMP-9	24	1.22	-1.01	1.50	1.68	1.21	2.34	1.38	-1.10	2.09
MMP-9	72	1.06	-1.22	1.37	9.46	6.01	14.89	9.82	5.85	16.49
MMP-9	168	1.10	-1.18	1.41	12.86	7.42	22.29	18.18	11.74	28.15
Laminin-γ2	24	-1.19	-2.27	1.61	-1.52	-2.78	1.18	-1.25	-1.61	1.03
Laminin-γ2	72	-2.13	-2.86	-1.56	18.12	9.10	35.81	7.32	5.19	10.32
Laminin-γ2	168	2.36	1.85	3.00	7.07	3.88	12.88	10.86	4.54	26.00
Laminin-5α3A	24	1.23	1.11	1.36	-2.78	-3.57	-2.22	-2.86	-3.57	-2.27
Laminin-5α3A	72	-1.15	-1.33	1.00	1.07	-1.23	1.42	2.69	2.16	3.35
Laminin-5α3A	168	1.12	1.03	1.23	-1.79	-2.70	-1.18	-1.27	-1.59	-1.02
Laminin-β3	24	1.09	-1.02	1.21	-3.70	-4.55	-2.94	-4.17	-4.55	-3.70
Laminin-β3	72	-1.12	-1.25	-1.01	1.10	-1.18	1.42	1.45	1.21	1.74
Laminin-β3	168	1.21	1.13	1.29	-1.25	-1.49	-1.04	-1.19	-1.52	1.08

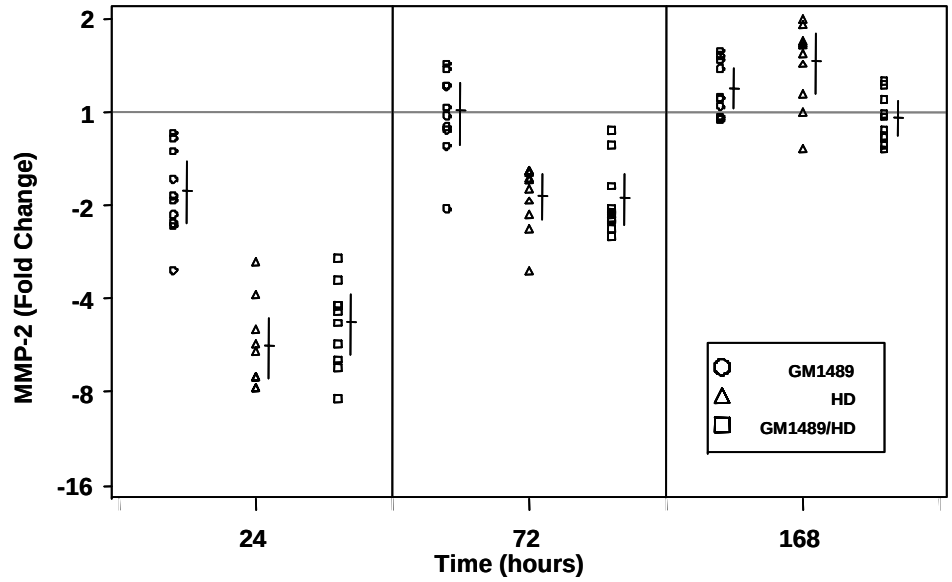

Figure 16. Effect of GM1489 on MMP-2 mRNA Levels. Fold change in MMP-2 mRNA levels in mouse ear skin pretreated with GM1489 only (circles), SM-exposed only (triangles), and pretreated with GM1489 and then SM-exposed (squares) at 24 h, 72 h, and 168 h post-exposure. Individual data points are indicated by the shapes. The horizontal dashes represent the geometric mean and the vertical lines represent the 95% confidence intervals.

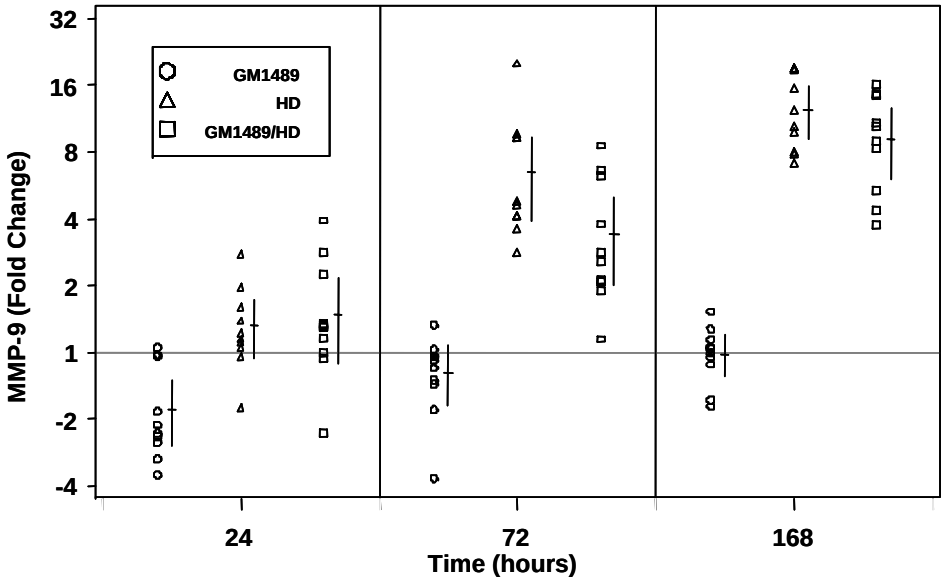

Figure 17. Effect of GM1489 on MMP-9 mRNA Levels. Fold change in MMP-9 mRNA levels in mouse ear skin pretreated with GM1489 only (circles), SM-exposed only (triangles), and pretreated with GM1489 and then SM-exposed (squares) at 24 h, 72 h, and 168 h post-exposure. Individual data points are indicated by the shapes. The horizontal dashes represent the geometric mean and the vertical lines represent the 95% confidence intervals.

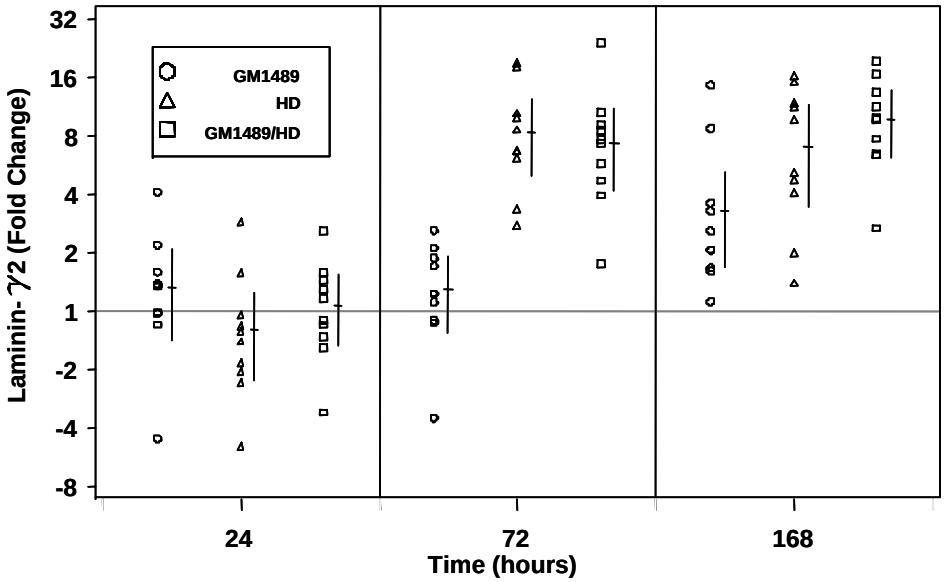

Figure 18. Effect of GM1489 on Laminin-γ2 mRNA Levels. Fold change in laminin-γ2 mRNA levels in mouse ear skin pretreated with GM1489 only (circles), SM-exposed only (triangles), and pretreated with GM1489 and then SM-exposed (squares) at 24 h, 72 h, and 168 h post-exposure. Individual data points are indicated by the shapes. The horizontal dashes represent the geometric mean and the vertical lines represent the 95% confidence intervals.

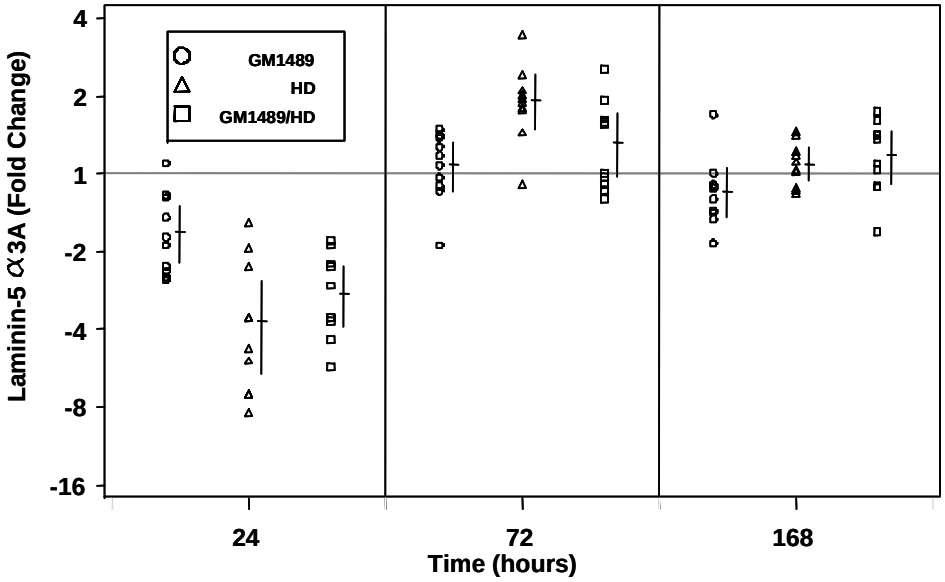

Figure 19. Effect of GM1489 on Laminin-5α3A mRNA Levels. Fold change in laminin-5α3A mRNA levels in mouse ear skin pretreated with GM1489 only (circles), SM-exposed only (triangles), and pretreated with GM1489 and then SM-exposed (squares) at 24 h, 72 h, and 168 h post-exposure. Individual data points are indicated by the shapes. The horizontal dashes represent the geometric mean and the vertical lines represent the 95% confidence intervals.

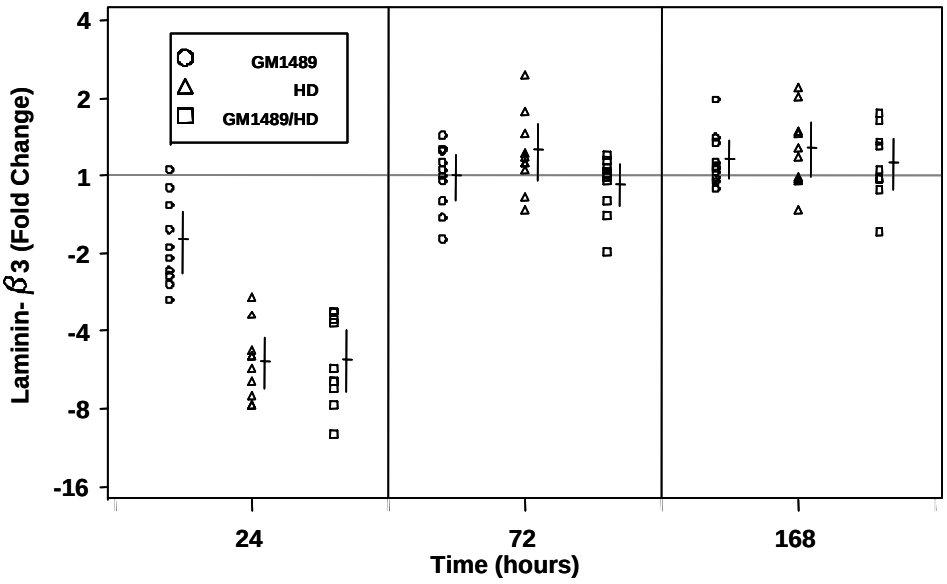

Figure 20. Effect of GM1489 on Laminin-β3 mRNA Levels. Fold change in laminin-β3 mRNA levels in mouse ear skin pretreated with GM1489 only (circles), SM-exposed only (triangles), and pretreated with GM1489 and then SM-exposed (squares) at 24 h, 72 h, and 168 h post-exposure. Individual data points are indicated by the shapes. The horizontal dashes represent the geometric mean and the vertical lines represent the 95% confidence intervals.

Table 10. Relative mRNA expression levels of MMP-2, MMP-9, laminin-γ2, laminin-5α3A, and laminin-β3 in mouse ear skin pretreated with GM1489 only, SM-exposed only, and pretreated with GM1489 and then SM-exposed at 24 h, 72 h, and 168 h post-exposure. Shaded values indicate significant difference between SM only and GM1489 + SM based on Tukey's multiple comparisons test performed at an overall 0.05 significance level.

Target Genes	Time (Hours)	GM1489 Only			SM Only			GM1489 + SM		
		Fold Change (Geometric Mean)	95% Confidence Interval		Fold Change (Geometric Mean)	95% Confidence Interval		Fold Change (Geometric Mean)	95% Confidence Interval	
			Lower	Upper		Lower	Upper		Lower	Upper
MMP-2	24	-1.82	-2.27	-1.45	-5.88	-7.14	-4.55	-4.76	-6.25	-3.85
MMP-2	72	-1.01	-1.27	1.25	-1.89	-2.22	-1.59	-1.92	-2.33	-1.59
MMP-2	168	1.19	1.03	1.38	1.43	1.15	1.78	-1.05	-1.19	1.08
MMP-9	24	-1.89	-2.70	-1.35	1.27	-1.08	1.73	1.39	-1.12	2.18
MMP-9	72	-1.28	-1.75	1.06	6.06	3.92	9.36	3.15	1.99	4.99
MMP-9	168	-1.04	-1.28	1.20	12.02	9.09	15.90	8.76	6.05	12.68
Laminin-γ2	24	1.21	-1.43	2.07	-1.37	-2.27	1.24	1.00	-1.52	1.52
Laminin-γ2	72	1.21	-1.30	1.89	7.81	4.96	12.28	6.81	4.18	11.11
Laminin-γ2	168	2.95	1.67	5.22	6.25	3.40	11.50	9.16	6.09	13.78
Laminin-5α3A	24	-1.72	-2.22	-1.33	-4.00	-5.88	-2.56	-2.94	-3.85	-2.27
Laminin-5α3A	72	1.07	-1.18	1.33	1.89	1.47	2.41	1.29	-1.03	1.71
Laminin-5α3A	168	-1.19	-1.47	1.05	1.09	-1.06	1.25	1.16	-1.10	1.46
Laminin-β3	24	-1.82	-2.38	-1.37	-5.26	-6.67	-4.17	-5.26	-7.14	-4.00
Laminin-β3	72	-1.02	-1.25	1.21	1.23	-1.05	1.58	-1.09	-1.32	1.11
Laminin-β3	168	1.16	-1.03	1.37	1.26	-1.02	1.61	1.10	-1.14	1.38

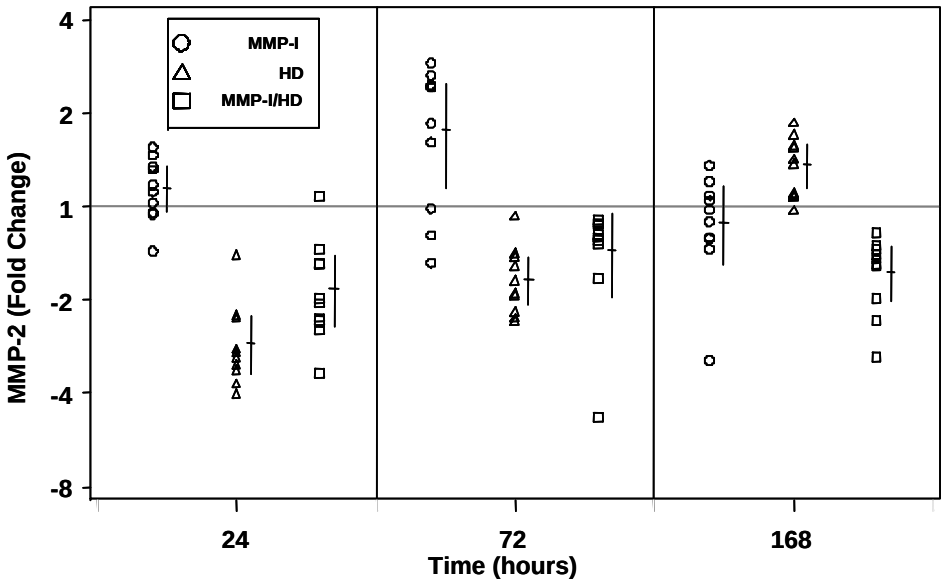

Figure 21. Effect of MMP-2/MMP-9 Inhibitor I (Inhibitor I) on MMP-2 mRNA Levels. Fold change in MMP-2 mRNA levels in mouse ear skin pretreated with Inhibitor I only (circles), SM-exposed only (triangles), and pretreated with Inhibitor I and then SM-exposed (squares) at 24 h, 72 h, and 168 h post-exposure. Individual data points are indicated by the shapes. The horizontal dashes represent the geometric mean and the vertical lines represent the 95% confidence intervals.

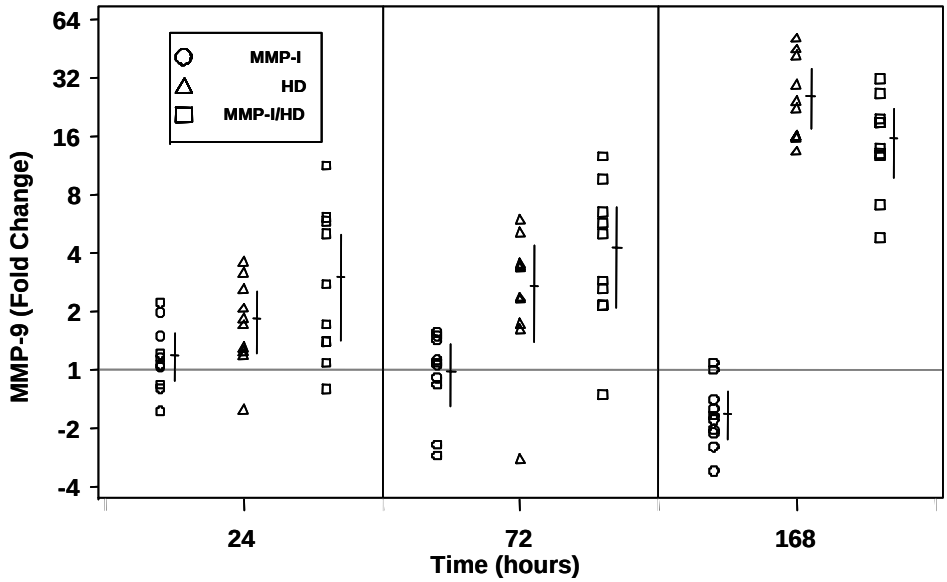

Figure 22. Effect of MMP-2/MMP-9 Inhibitor I (Inhibitor I) on MMP-9 mRNA Levels. Fold change in MMP-9 mRNA levels in mouse ear skin pretreated with Inhibitor I only (circles), SM-exposed only (triangles), and pretreated with Inhibitor I and then SM-exposed (squares) at 24 h, 72 h, and 168 h post-exposure. Individual data points are indicated by the shapes. The horizontal dashes represent the geometric mean and the vertical lines represent the 95% confidence intervals.

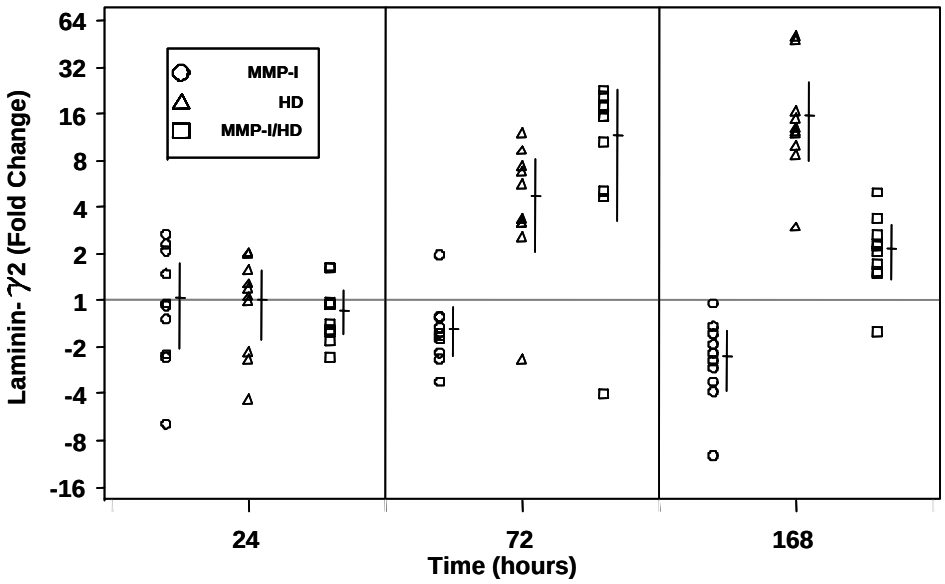

Figure 23. Effect of MMP-2/MMP-9 Inhibitor I (Inhibitor I) on Laminin-γ2 mRNA Levels. Fold change in laminin-γ2 mRNA levels in mouse ear skin pretreated with Inhibitor I only (circles), SM-exposed only (triangles), and pretreated with Inhibitor I and then SM-exposed (squares) at 24 h, 72 h, and 168 h post-exposure. Individual data points are indicated by the shapes. The horizontal dashes represent the geometric mean and the vertical lines represent the 95% confidence intervals.

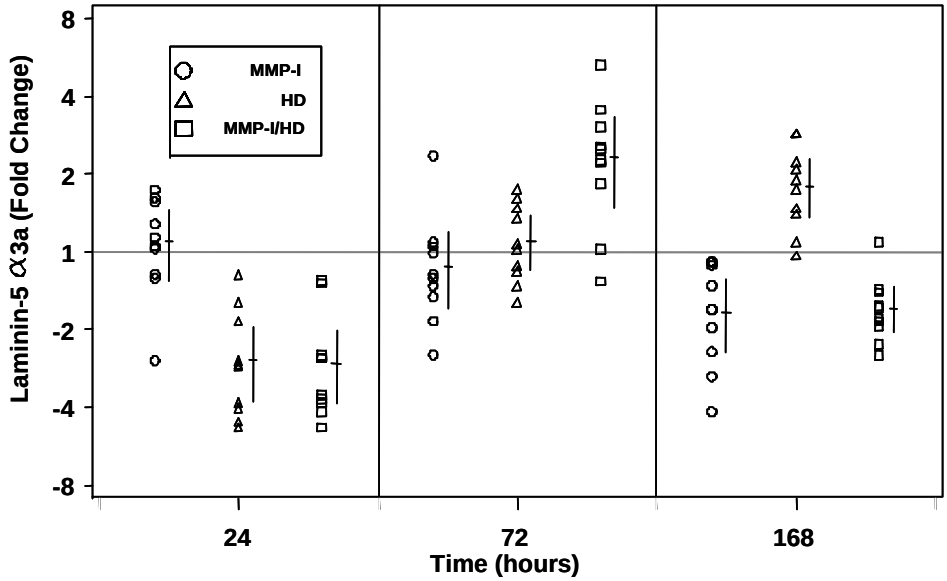

Figure 24. Effect of MMP-2/MMP-9 Inhibitor I (Inhibitor I) on Laminin-5α3A mRNA Levels. Fold change in laminin-5α3A mRNA levels in mouse ear skin pretreated with Inhibitor I only (circles), SM-exposed only (triangles), and pretreated with Inhibitor I and then SM-exposed (squares) at 24 h, 72 h, and 168 h post-exposure. Individual data points are indicated by the shapes. The horizontal dashes represent the geometric mean and the vertical lines represent the 95% confidence intervals.

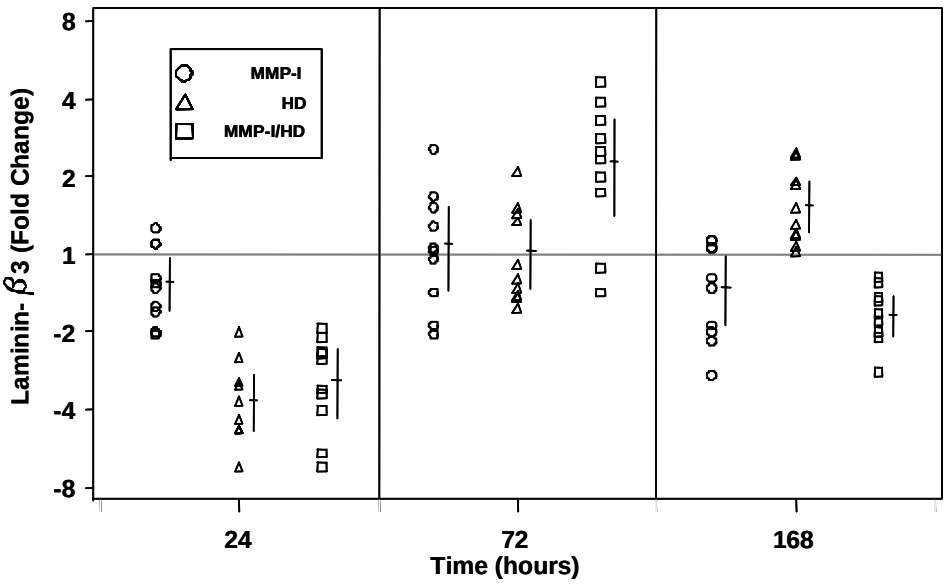

Figure 25. Effect of MMP-2/MMP-9 Inhibitor I (Inhibitor I) on Laminin-β3 mRNA Levels. Fold change in laminin-β3 mRNA levels in mouse ear skin pretreated with Inhibitor I only (circles), SM-exposed only (triangles), and pretreated with Inhibitor I and then SM-exposed (squares) at 24 h, 72 h, and 168 h post-exposure. Individual data points are indicated by the shapes. The horizontal dashes represent the geometric mean and the vertical lines represent the 95% confidence intervals.

Table 11. Relative mRNA expression levels of MMP-2, MMP-9, laminin-γ2, laminin-5α3A, and laminin-β3 in mouse ear skin pretreated with MMP-2/MMP-9 Inhibitor I (Inhibitor I) only, SM-exposed only, and pretreated with Inhibitor I and then SM-exposed at 24 h, 72 h, and 168 h post-exposure. Shaded values indicate significant difference between SM only and Inhibitor I + SM based on Tukey's multiple comparisons test performed at an overall 0.05 significance level.

Target Genes	Time (Hours)	Inhibitor I Only			SM Only			Inhibitor I + SM		
		Fold Change (Geometric Mean)	95% Confidence Interval		Fold Change (Geometric Mean)	95% Confidence Interval		Fold Change (Geometric Mean)	95% Confidence Interval	
			Lower	Upper		Lower	Upper		Lower	Upper
MMP-2	24	1.14	-1.04	1.35	-2.78	-3.45	-2.27	-1.89	-2.44	-1.43
MMP-2	72	1.68	1.14	2.48	-1.72	-2.08	-1.45	-1.43	-1.96	-1.04
MMP-2	168	-1.15	-1.54	1.16	1.35	1.15	1.59	-1.64	-2.04	-1.35
MMP-9	24	1.15	-1.16	1.53	1.74	1.20	2.53	2.64	1.40	4.99
MMP-9	72	-1.08	-1.54	1.34	2.43	1.37	4.31	3.78	2.08	6.90
MMP-9	168	-1.72	-2.27	-1.30	24.93	17.53	35.44	14.71	9.74	22.23
Laminin-γ2	24	-1.10	-2.08	1.72	-1.08	-1.82	1.57	-1.20	-1.64	1.15
Laminin-γ2	72	-1.59	-2.27	-1.11	4.07	2.06	8.05	8.65	3.26	22.98
Laminin-γ2	168	-2.50	-3.85	-1.59	14.16	7.89	25.42	2.04	1.38	3.03
Laminin-5α3A	24	1.06	-1.32	1.46	-2.70	-3.85	-1.96	-2.78	-3.85	-2.00
Laminin-5α3A	72	-1.19	-1.67	1.19	1.08	-1.18	1.38	2.21	1.48	3.31
Laminin-5α3A	168	-1.79	-2.44	-1.28	1.76	1.35	2.30	-1.67	-2.04	-1.37
Laminin-β3	24	-1.32	-1.67	-1.03	-3.70	-4.76	-2.94	-3.23	-4.35	-2.33
Laminin-β3	72	1.05	-1.37	1.52	1.00	-1.35	1.35	2.15	1.40	3.32
Laminin-β3	168	-1.39	-1.92	-1.02	1.52	1.21	1.92	-1.75	-2.08	-1.45

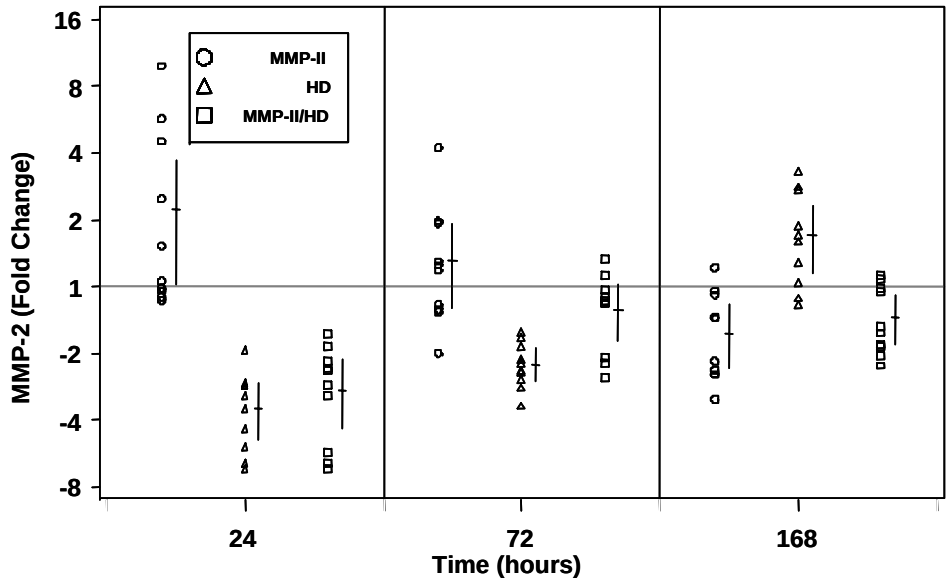

Figure 26. Effect of MMP-2/MMP-9 Inhibitor II (Inhibitor II) on MMP-2 mRNA Levels. Fold change in MMP-2 mRNA levels in mouse ear skin pretreated with Inhibitor II only (circles), SM-exposed only (triangles), and pretreated with Inhibitor II and then SM-exposed (squares) at 24 h, 72 h, and 168 h post-exposure. Individual data points are indicated by the shapes. The horizontal dashes represent the geometric mean and the vertical lines represent the 95% confidence intervals.

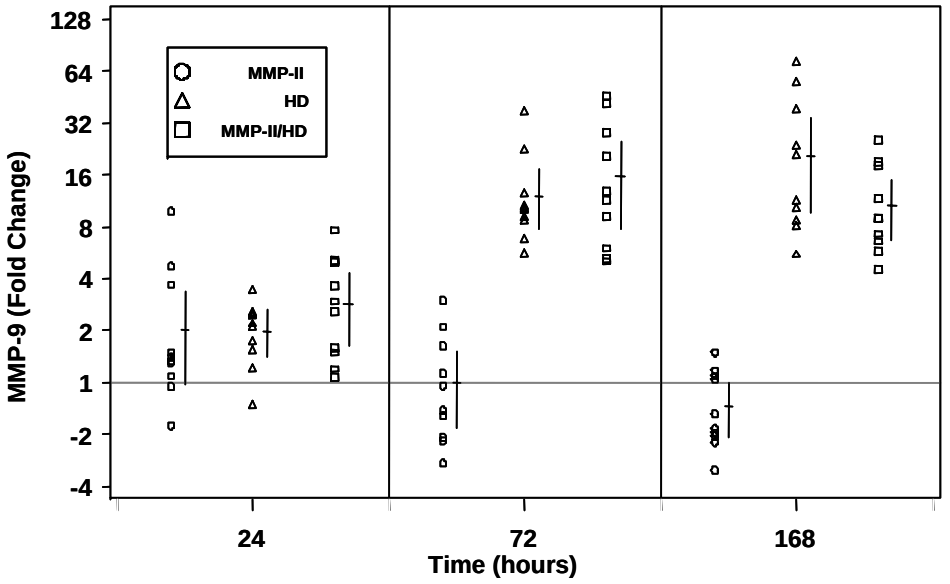

Figure 27. Effect of MMP-2/MMP-9 Inhibitor II (Inhibitor II) on MMP-9 mRNA Levels. Fold change in MMP-9 mRNA levels in mouse ear skin pretreated with Inhibitor II only (circles), SM-exposed only (triangles), and pretreated with Inhibitor II and then SM-exposed (squares) at 24 h, 72 h, and 168 h post-exposure. Individual data points are indicated by the shapes. The horizontal dashes represent the geometric mean and the vertical lines represent the 95% confidence intervals.

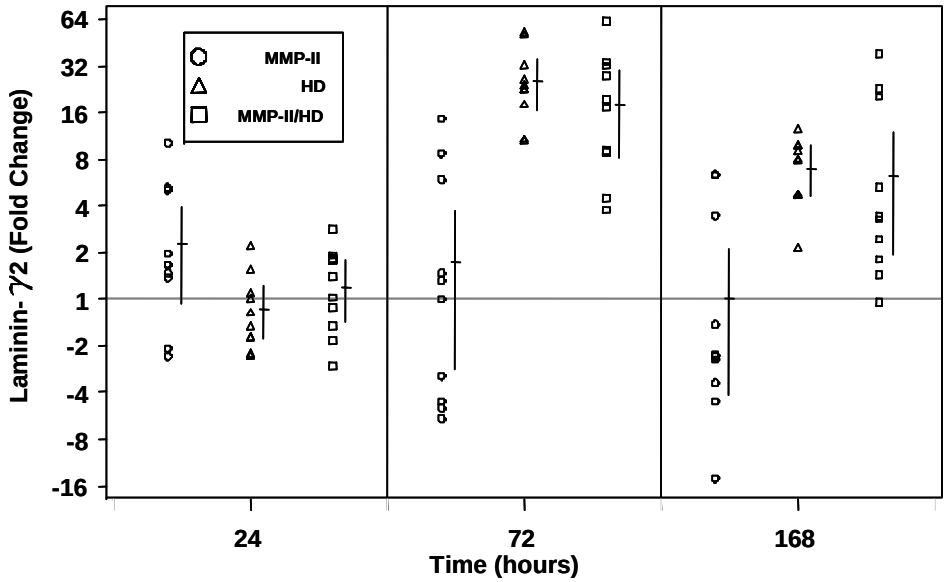

Figure 28. Effect of MMP-2/MMP-9 Inhibitor II (Inhibitor II) on Laminin-γ2 mRNA Levels. Fold change in laminin-γ2 mRNA levels in mouse ear skin pretreated with II only (circles), SM-exposed only (triangles), and pretreated with Inhibitor II and then SM-exposed (squares) at 24 h, 72 h, and 168 h post-exposure. Individual data points are indicated by the shapes. The horizontal dashes represent the geometric mean and the vertical lines represent the 95% confidence intervals.

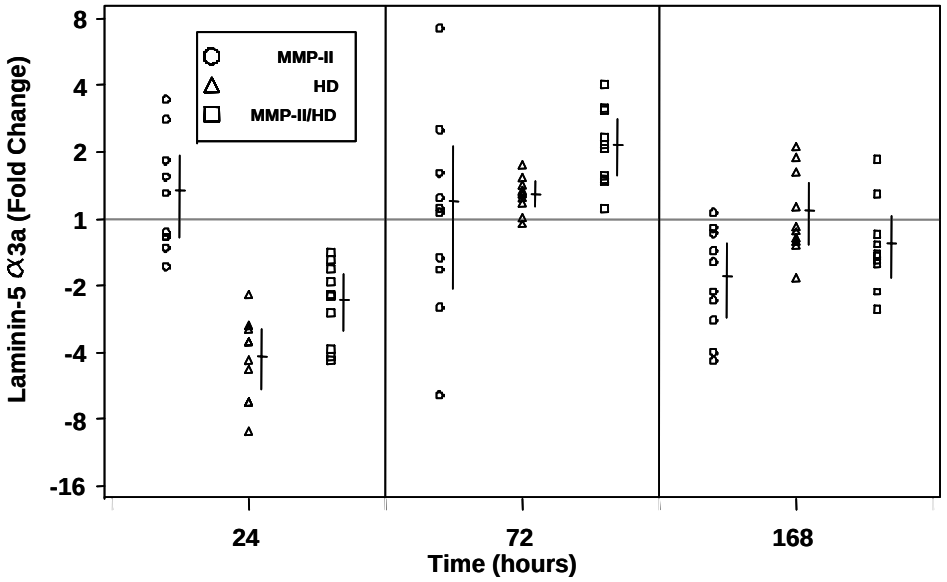

Figure 29. Effect of MMP-2/MMP-9 Inhibitor II (Inhibitor II) on Laminin-5α3A mRNA Levels. Fold change in laminin-5α3A mRNA levels in mouse ear skin pretreated with Inhibitor II only (circles), SM-exposed only (triangles), and pretreated with Inhibitor II and then SM-exposed (squares) at 24 h, 72 h, and 168 h post-exposure. Individual data points are indicated by the shapes. The horizontal dashes represent the geometric mean and the vertical lines represent the 95% confidence intervals.

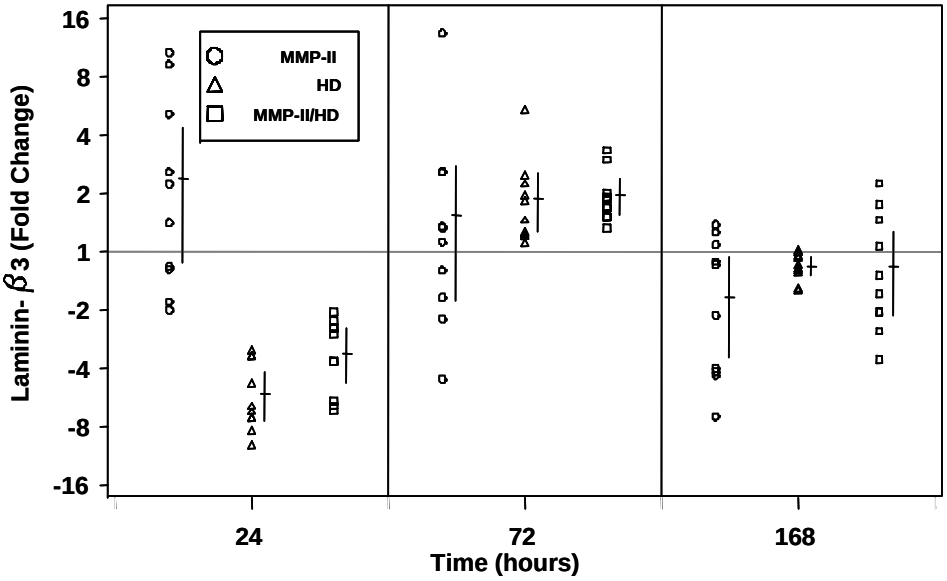

Figure 30. Effect of MMP-2/MMP-9 Inhibitor II (Inhibitor II) on Laminin-β3 mRNA Levels. Fold change in laminin-β3 mRNA levels in mouse ear skin pretreated with Inhibitor II only (circles), SM-exposed only (triangles), and pretreated with Inhibitor II and then SM-exposed (squares) at 24 h, 72 h, and 168 h post-exposure. Individual data points are indicated by the shapes. The horizontal dashes represent the geometric mean and the vertical lines represent the 95% confidence intervals.

Table 12. Relative mRNA expression levels of MMP-2, MMP-9, laminin-γ2, laminin-5α3A, and laminin-β3 in mouse ear skin pretreated with MMP-2/MMP-9 Inhibitor II (Inhibitor II) only, SM-exposed only, and pretreated with Inhibitor II and then SM-exposed at 24 h, 72 h, and 168 h post-exposure. Shaded values indicate significant difference between SM only and Inhibitor II + SM based on Tukey's multiple comparisons test performed at an overall 0.05 significance level.

Target Genes	Time (Hours)	Inhibitor II Only			SM Only			Inhibitor II + SM		
		Fold Change (Geometric Mean)	95% Confidence Interval		Fold Change (Geometric Mean)	95% Confidence Interval		Fold Change (Geometric Mean)	95% Confidence Interval	
			Lower	Upper		Lower	Upper		Lower	Upper
MMP-2	24	1.95	1.02	3.69	-3.70	-5.00	-2.70	-3.03	-4.35	-2.13
MMP-2	72	1.23	-1.27	1.90	-2.27	-2.70	-1.92	-1.32	-1.75	1.03
MMP-2	168	-1.69	-2.33	-1.20	1.63	1.14	2.31	-1.43	-1.82	-1.11
MMP-9	24	1.80	-1.02	3.34	1.91	1.39	2.62	2.65	1.63	4.31
MMP-9	72	-1.10	-1.85	1.51	11.48	7.70	17.11	13.84	7.64	25.07
MMP-9	168	-1.45	-2.08	-1.01	18.08	9.63	33.97	10.07	6.71	15.12
Laminin-γ2	24	1.91	-1.08	3.92	-1.20	-1.79	1.21	1.12	-1.41	1.78
Laminin-γ2	72	1.14	-2.86	3.70	24.01	16.28	35.41	15.66	8.11	30.25
Laminin-γ2	168	-1.41	-4.17	2.09	6.67	4.57	9.72	4.82	1.94	11.95
Laminin-5α3A	24	1.26	-1.22	1.92	-4.35	-5.88	-3.13	-2.38	-3.23	-1.79
Laminin-5α3A	72	1.01	-2.08	2.13	1.29	1.13	1.46	2.10	1.57	2.81
Laminin-5α3A	168	-1.92	-2.78	-1.30	1.05	-1.32	1.44	-1.33	-1.85	1.04
Laminin-β3	24	1.94	-1.15	4.35	-5.56	-7.69	-4.17	-3.45	-4.76	-2.50
Laminin -β3	72	1.24	-1.82	2.78	1.79	1.27	2.52	1.91	1.54	2.35
Laminin -β3	168	-1.92	-3.57	-1.06	-1.19	-1.33	-1.06	-1.30	-2.13	1.27

Table 13. Relative Gene Expression Levels Following Compound Pre-Treatment + SM as Compared to SM-Only

Compound	Time Point (h)	MMP-2	MMP-9	Laminin-γ2	Laminin5-α3A	Laminin-β3
Ilomastat	24	NC[1]	NC[1]	NC[1]	NC[1]	NC[1]
	72	NC[1]	NC[1]	↓	↑[3]	NC[1]
	168	NC[1]	NC[1]	NC[1]	NC[1]	NC[1]
GM1489	24	NC[1]	NC[1]	NC[1]	NC[1]	NC[1]
	72	NC[1]	↓	NC[1]	NC[1]	NC[1]
	168	↓[2]	NC[1]	NC[1]	NC[1]	NC[1]
MMP-2/MMP-9 Inhibitor I	24	NC[1]	NC[1]	NC[1]	NC[1]	NC[1]
	72	NC[1]	NC[1]	NC[1]	↑	↑
	168	↓	NC[1]	↓	↓	↓
MMP-2/MMP-9 Inhibitor II	24	NC[1]	NC[1]	NC[1]	↑	NC[1]
	72	NC[1]	NC[1]	NC[1]	NC[1]	NC[1]
	168	NC[1]	NC[1]	NC[1]	NC[1]	NC[1]

[1]NC = No change
[2]↓ = Significantly decreased gene expression
[3]↑ = Significantly increased gene expression

Mouse Epidermal Keratinocytes (MEK): Establishment in Culture and Characteristics

Figure 31

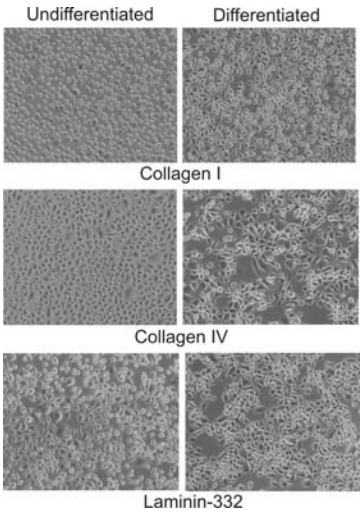

MEK have been traditionally difficult to grow in primary culture and to subculture. Using the method of Hager[26] we have perfected the techniques of isolation, primary culture, cryopreservation and revival, and long term culture over many passages. We seeded and differentiated MEK on cell cultureware coated with three different extracellular matrices, Collagen I, collagen IV, and laminin-332, to determine culture characteristics under these conditions. As shown in Figure 31, MEK grew well on all three surfaces with a greater propensity towards uniform growth to confluence on collagen IV. All three matrices supported differentiation, with migration and stratification observed in the cultures upon increasing [Ca^{++}] in serum-free culture medium to 0.15 mM for 72 hr. RT-PCR indicated that differentiating conditions produced a relative increase in mouse keratin I (MK1) and profilaggrin, typical markers of keratinocyte differentiation (Fig 32). Cells grown on laminin-332 displayed the highest increase in mRNA, relative to undifferentiated control, of the markers examined.

Effect of Attachment Matrix upon Relative mRNA Expression of Differentiation Markers

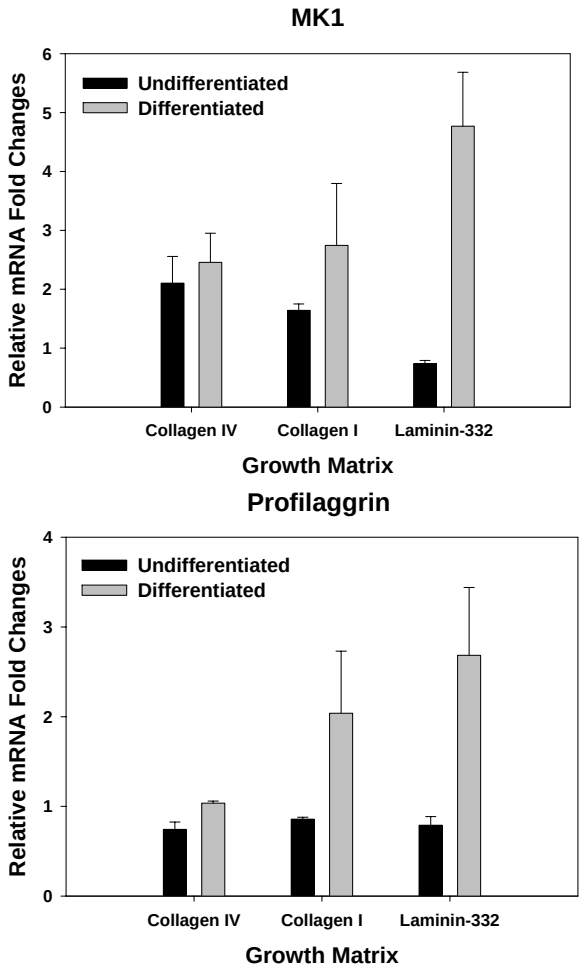

Figure 32 RT-PCR for mouse keratin I (MK1, upper panel) and profilaggrin (Lower panel) on keratinocyte mRNA from keratinocytes grown on either collagen IV, collagen I or laminin-332. Cells were either undifferentiated (grey bars) or differentiated (black bars). Standard error bars are shown

In summary, these *in vitro* studies (1) demonstrate our ability to isolate, culture, subculture, and differentiate MEK, (2) show that MEK grow well on various natural matrices with a tendency towards a morphology more akin to the resting *in vivo* situation when seeded upon collagen IV, and (3) indicate that while differentiation can occur upon all three matrices, relative mRNA levels of the key differentiation markers, MK1 and profilaggrin are induced to a greater extent in cells grown on laminin-332.

KEY RESEARCH ACCOMPLISHMENTS

- Mouse ear tissue has been collected and stored for both the initial time course study and the compound evaluation study.
- Gene expression analysis has been completed for the time course study and for the compound evaluation study.
- Gene expression analysis has been completed for the evaluation of Ilomastat, GM1489, MMP-2/MMP-9 Inhibitor I, and MMP-2/MMP-9 Inhibitor II pre-treatment.
- An *in vitro* mouse keratinocyte culture system was optimized for potential testing of anti-vesicant agents.

REPORTABLE OUTCOMES

- A database of SM-induced alterations in the gene expression of MMP-2, MMP-9, laminin-γ2, laminin5-α3A, and laminin-β3 with and without compound pre-treatment

SUMMARY OF RESULTS AND DISCUSSION

In conclusion, the statement of work was completed in its entirety. This proposal was essentially divided into three sections which will be discussed separately:

(1) Time course study

Rationale: The time course study was initiated for several reasons. Firstly, much work has been done involving the early (6, 12, 24 h) timepoints of the MEVM model, but little in the way of later (72, 168h) timepoints, when a second wave of inflammation occurs and repair processes begin. Since EB and SM-induced skin injury have similar morphologic consequences, we decided to compare biomarkers of EB injury to the MEVM. These biomarkers include the three polypeptide chains (laminin-α3, laminin-β3, and laminin-γ2) that together form laminin-332, a glycoprotein imperative to both keratinocyte adhesion in the intact skin and epithelial sheet migration in wounded skin. Other biomarkers are MMP-2 and MMP-9, a pair of gelatinases that are known to digest collagen IV, the major structural protein of the basement membrane and whose integrity must be maintained in order for skin to remain intact.

Summary of Results: For the time course study, gene expression levels were determined using real-time PCR in mouse ear tissue samples at 6, 12, 24, and 72 h post-exposure to SM. Laminin-γ2 expression levels initially decreased at 6 and 12 h post-exposure followed by a slight increase at 24 h and a **significant** increase 72 h post-exposure (to approximately 6-fold). Laminin5-α3A expression levels were decreased at 6, 12, and 24 h post-exposure followed by a minimal increase at 72 h post-exposure. Laminin-β3 expression levels initially decreased at 6, 12, and 24 h post-exposure followed by a slight increase at 72 h.

Discussion: Skin wound repair in the MEVM followed the normal progression of wound repair of thermal burns which includes inflammation, tissue formation, and tissue remodeling. Part of the process involves repair of the normal keratinocyte anchoring system

that attaches basal keratinocytes to the underlying dermis. This attachment helps maintain the integrity of skin to the externally applied force. There are many structural proteins involved in these interactions, but one of the major anchoring proteins is laminin-332, the major constituent of the anchoring filaments in skin basement membranes. The filaments attach to the hemidesmosomes in the keratinocyte basal layer, via integrin α6β4[28] and collagen XVII[29]. The other end of the laminin 5 molecule binds to type VII collagen in anchoring fibrils in the underlying dermis[30]. Our results show that compared to laminin-α3 and laminin-β3, laminin-γ2 mRNA is specifically upregulated as time after SM exposure increases. We explain this observation in terms of the migratory role of laminin-γ2. In addition to the structural, adhesive function of laminin-332 there are two lines of evidence which show that the molecule can serve as a migratory matrix for keratinocytes. The first addresses migration of cells directly on purified laminin-332[31;32]. The second is derived from studies on an epithelial cell "scatter factor," which was termed ladsin. This molecule is actually the same as laminin-332 and facilitates epithelial tumor cell migration[33;34]. Interestingly, the switch from cell adhesion to cell migration occurs with a change from α6β4 integrin-laminin-332 interactions to α3β1 integrin-laminin-332 interactions, in both cell culture and *in vivo* wound healing[35]. There is also a correlation between laminin-332 expression and malignant epithelial carcinoma invasiveness: laminin-332 appears at the invading edge of the migrating cells[31;32]. There is a specific intracellular accumulation of laminin-γ2 in such cells[36]. Furthermore, in some pancreatic carcinoma cells, the laminin-γ2 is secreted extracellularly, and is postulated to exist as a monomer[37]. The ramifications of monomeric laminin γ2 are not totally understood, but it has been found that, if the polypeptide is further processed to smaller forms by MMPs, then epithelial cell migration is enhanced[37;38]. The evidence suggests that, at least in the rat, one 30 kDa fragment called DIII contains epidermal growth factor-like motifs and can bind the EGF-receptor and induce its phosphorylation[39]. The end result is that the interaction of EGF receptor with the laminin-γ2 fragment stimulates cell scattering and migration. We speculate that laminin-γ2 is preferentially upregulated at the leading edge of the epithelial sheet that moves over exposed dermis in healing skin. The keratinocytes make it themselves presumably to cover receptors that might bind the moving cells, causing them to adhere instead. This would enhance covering the wound bed and hence wound repair.

Recommendations: The fact that the laminin-γ2 chain is preferentially expressed during wound repair in the MEVM raises the possibility that enhancing its production might speed up wound repair with the absence of scarring. It is suggested that endogenous laminin-332 be applied to SM-wounded ears to see if healing occurs faster. It is also suggested that basic observations and similar experiments to those in this report be performed on even longer timepoints after SM exposure (e.g. 1-6 months) since there appears to be recurring inflammatory events that contribute to the long-term effects of SM exposure in humans. Some of these effects include late skin lesions were hyperpigmentation, dry skin, atrophy, and hypopigmentation[40]. It is also suggested that the potential switch from α6β4 integrin-laminin-332 interactions to α3β1 integrin-laminin-332 interactions be examined as markers of the end of migration and the stabilization of the epithelial sheet over the wound bed.

(2) Compound evaluation study

Rationale: In normal situations the MMPs function in the turnover of extracellular matrix components, such as collagens, proteoglycans, elastin, laminin, fibronectin, and other glycoproteins. They are thought to play important roles in embryo development, morphogenesis, angiogenesis, and tissue involution. Expression of MMPs in healthy tissues is low, but their production is markedly increased in chronic wounding conditions such as EB. Their increased production can be anticipated after SM treatment as well since we recently reported upregulation of MMP-9 mRNA levels were elevated SM treated mouse skin 4.4, 6.5, and 27.8-fold for the 24, 72, and 168hr post-treated samples, respectively[41]. Since proteases have been implicated in the pathophysiology of SM-induced blistering, the effectiveness of synthetic MMP inhibitors may be effective therapeutic agents against SM-induced tissue injury. In fact, several recent reports show some success in the use of protease inhibitors both *in vitro* in cell culture[42] and *in vivo* in a mouse model[24;25]. Based on our observations to date, candidate synthetic MMP inhibitors (Ilomastat, GM1489, MMP-2/MMP-9 Inhibitor I, and MMP-2/MMP-9 Inhibitor II) were selected for evaluation of their ability to protect against SM injury in the mouse ear skin model.

Summary of Results:

In this study of the time course of SM-induced dermal changes in MMP expression, our results in the mouse ear vesicant injury model are similar to those in swine where MMP–9

mRNA levels increased within 48 h of injury[43]. We have extended these observations by showing that over a 168 h period after SM-injury, MMP–9 mRNA and protein levels increased. In contrast, no increases in mRNA and protein for MMP–2 occurred over the same time period. Gelatinase activity was increased during the 168 h period. However, the specific type of gelatinase contributing to increased activity could not be determined from the assay used. These results suggest that MMP–9 and MMP–2 are differentially expressed during the first 168 h of SM-induced dermal injury[41].

The results for pre-treatment with various protease inhibitors, followed by SM exposure were variable, but "Inhibitor I" affected the most genes. Pre-treatment with Ilomastat in conjunction with SM exposure significantly decreased laminin-γ2 expression at 72 h and significantly increased laminin332-α3A expression at 72 h as compared to SM-only (no drug compound pre-treatment). This coincided with a slightly improved Draize Score at 72 h with Ilomastat pre-treatment as compared to the other compounds. Pre-treatment with GM1489 in conjunction with SM exposure significantly decreased MMP-9 expression at 72 h and decreased MMP-2 expression at 7 days as compared to SM-only. Pre-treatment with MMP-2/MMP-9 Inhibitor I in conjunction with SM exposure significantly decreased MMP-2, laminin-γ2, laminin332-α3A, and laminin-β3 expression at 7 days and increased laminin-β3 and laminin332-α3A expression at 72 h as compared to SM-only. Pre-treatment with MMP-2/MMP-9 Inhibitor II in conjunction with SM exposure significantly increased laminin332-α3A expression at 24 h as compared to SM-only.

Discussion:

The specific aim of the time course study was to determine whether MMP and MMP substrate gene expression levels are altered over time (6, 12, 24, 72, 168 h) in mouse ear skin topically exposed to liquid SM. The inflammatory changes determined by skin Draize score and histopathology were similar to previous observations in the mouse ear model of SM-induced injury[24]. The histopathology of the mouse skin to SM is also similar to the response in humans[44], indicating that the mouse is a good model of the human disorder. The pertinent changes were early edema and infiltration of skin by leukocytes followed by dyskeratotic basal cells and ketatinocytes with contracted hyperchromatic nuclei at 168 h. Necrosis observed on the opposite side of the ear from the site of SM application is likely due to the presumed diffusion of SM

through the cartilage. The progressive tissue injury paralleled the increased gelatinase activity and elevated levels of MMP–9 mRNA and protein.

Differential expression of MMP–2 and MMP–9 has been observed in another model of epithelial injury. During wound healing in human oral mucosa, MMP–9 mRNA is markedly increased whereas MMP–2 levels remain stable during healing up to 168 h[45] . This may be due in part to differing levels of expression of the two MMPs by epithelial cells. Another explanation is that the differential expression may be due to changing populations of cells over the observed period. Neutrophils, the first line of defense in tissue injury, produce MMP-9, but not MMP–2[46]. In contrast, mononuclear leukocytes produce MMP–2 constitutively and MMP–9 *de novo* after stimulation. Thus, differential expression of MMPs during the course of SM-induced injury may be explained by changing types of endogenous or recruited cell populations. If increased MMP-9 is deleterious to tissue, why then is it specifically upregulated in response to SM treatment? We speculate that the sustained expression of MMP–9 for 168 h may serve to resolve SM-induced injury rather than enhance it. Our speculation arises from the observation that wounded MMP-9 null mice heal more slowly than controls, suggestive of a beneficial affect of MMP-9 in wound healing[47]. A possible mechanism to explain this observation would be MMP-9 stimulation of TGF–β as a secondary messenger. It is known that cell surface localized MMP–9 activates TGF–β which in turn stimulates a host of wound repair proteins[47]. These observations raise intriguing questions about the strategy of using MMP inhibitors[48]. In theory, MMP–9 inhibitors may either decrease the MMP-9 induced injury in the early phase of SM-wounding or interfere with the later MMP-9 mediated repair of vesicant wounds. Further studies may resolve this discrepancy.

The aim of the compound evaluation study was to determine the effectiveness of topically delivered synthetic MMP inhibitors, Ilomastat, GM1489, MMP-2/MMP-9 Inhibitor I, and MMP-2/MMP-9 Inhibitor II, to protect against SM injury. Protection was quantitatively assessed by measuring MMP and MMP substrate gene expression levels with subsequent correlation to histopathological damage in tissues harvested at 24 h, 72 h and 168 hours after SM challenge. The data was mostly inconsistent and only pre-treatment with MMP-2/MMP-9 Inhibitor I showed promise with reducing the transcription of a number of genes at multiple

timepoints. However, this could not be correlated with lessened tissue damage. We conclude either the strategy doesn't work or the inhibitor did not reach its target.

Recommendations:.

We believe the possible use of protease inhibitors as potential countermeasures of SM-induced skin injury warrants further investigation. We suggest that alternate formulations be tested to ensure the compounds reach the intended targets (ie penetrate the skin barrier). We consider that vesicant injury is a multi-step process which loosely may be divided into five phases: 1) Alkylation, with immediate protein and DNA damage 2) inflammation 3) protease activation and secondary structural damage 4) apoptosis and cellular necrosis and 5) tissue repair. Countermeasures have been aimed at some of these specific phases. Bioscavengers such as mercaptopyridine compounds target phase 1. Protease inhibitors may be used for phase 3. The vanilloids target the inflammation phase and ZVAD-fmk target apoptosis. We would suggest a multi-targeted countermeasure approach that targets multiple steps in the wound injury and repair process (e.g. combine treatments). We also believe longer timepoints need to be examined to observe complete healing of the wounded area.

Preliminary results raise the possibility of MMPs as mediators of dermal injury and needs to be examined further. Recent studies using MMP–9 null mice suggesting a role for MMP–9 in resolution of tissue injury imply a possible beneficial role for MMP–9. Additional SM-exposure studies using mice genetically lacking MMP–9 may elucidate the role of MMP–9 in degradation and repair of tissues in SM-induced injury.

(3) *In vitro* mouse keratinocyte study

Rationale: There is great interest in reducing the numbers of animals used in compound evaluation studies, so alternative *in vitro* methods are currently under investigation. One drawback to mouse *in vitro* studies has been the fact that compared to human cultures, mouse keratinocytes are difficult to grow as primary cultures. Furthermore, their use as subcultures has been nearly impossible. Therefore we investigated the possibility of substituting murine cultures in place of the MEVM.

Summary of Results and Discussion: Using a method for growing newborn mouse keratinocytes, we have passaged cells at least 13 times[26]. We were able to differentiate them and

identified key biomarkers that correspond to *in vivo* biomarkers (MK1 and profilaggrin).. We found that the viability of mouse keratinocyte cultures in part is determined by the matrix on which they are grown with collagen IV the best matrix for resting keratinocytes and laminin-332 the best for differentiation of keratinocytes.

Recommendations: We believe this system has great promise in reducing the numbers of live animals used in compound evaluation studies and recommend it be developed further. Additional biomarkers need to be identified and compared to the biomarker levels in fresh animal skin. Optimal conditions need to be established to further mimic the *in vivo* situation. Then the cultures need to be treated with SM and compared to the MEVM model.

This research addresses milestone objectives of the Joint Service Chemical and Biological Defense Program Defense Technology Objective (DTO) CB.30 (Medical Countermeasures for Vesicant Agents II). A primary objective of the DTO is to demonstrate safe and effective pharmacological countermeasures to prevent or decrease by 80% the severity of injuries caused by SM exposure. This study determined the *in vivo* efficacy of candidate protease inhibitor therapies in an animal model.

Reference List

(1) Papirmeister B, Gross CL, Petrali J et al. Pathology produced by sulfur mustard in human skin grafts on athymic nude mice I. Gross and light microscopic changes. J Toxicol Cutan OcularToxicol 1984; 3:371-408.

(2) Aumailley M, Bruckner-Tuderman L, Carter WG et al. A simplified laminin nomenclature. Matrix Biol 2005; 24(5):326-332.

(3) Gerecke DR, Wagman DW, Champliaud MF et al. The complete primary structure for a novel laminin chain, the laminin B1k chain. J Biol Chem 1994; 269(15):11073-11080.

(4) Chen M, Marinkovich MP, Jones JC et al. NC1 domain of type VII collagen binds to the beta3 chain of laminin 5 via a unique subdomain within the fibronectin-like repeats. J Invest Dermatol 1999; 112(2):177-183.

(5) Brittingham R, Uitto J, Fertala A. High-affinity binding of the NC1 domain of collagen VII to laminin 5 and collagen IV. Biochem Biophys Res Commun 2006; 343(3):692-699.

(6) Christiano AM, Uitto J. Polymorphism of the human genome: markers for genetic linkage analyses in heritable diseases of the skin. J Invest Dermatol 1992; 99(5):519-523.

(7) Petrali JP, Oglesby-Megee S. Toxicity of mustard gas skin lesions. Microsc Res Tech 1997; 37(3):221-228.

(8) Monteiro-Riviere NA, Inman AO, Babin MC et al. Immunohistochemical characterization of the basement membrane epitopes in bis(2-chloroethyl) sulfide-induced toxicity in mouse ear skin. J Appl Toxicol 1999; 19(5):313-328.

(9) Matsui C, Pereira P, Wang CK et al. Extent of laminin-5 assembly and secretion effect junctional epidermolysis bullosa phenotype. J Exp Med 1998; 187(8):1273-1283.

(10) Fine JD, Eady RA, Bauer EA et al. Revised classification system for inherited epidermolysis bullosa: Report of the Second International Consensus Meeting on diagnosis and classification of epidermolysis bullosa. J Am Acad Dermatol 2000; 42(6):1051-1066.

(11) Ryan MC, Tizard R, VanDevanter DR et al. Cloning of the LamA3 gene encoding the alpha 3 chain of the adhesive ligand epiligrin. Expression in wound repair. J Biol Chem 1994; 269(36):22779-22787.

(12) Vailly J, Verrando P, Champliaud MF et al. The 100-kDa chain of nicein/kalinin is a laminin B2 chain variant. Eur J Biochem 1994; 219(1-2):209-218.

(13) Marinkovich MP, Lunstrum GP, Keene DR et al. The dermal-epidermal junction of human skin contains a novel laminin variant. J Cell Biol 1992; 119(3):695-703.

(14) Uitto J, Richard G. Progress in epidermolysis bullosa: genetic classification and clinical implications. Am J Med Genet C Semin Med Genet 2004; 131C(1):61-74.

(15) Monteiro-Riviere NA, Inman AO. Ultrastructural characterization of sulfur mustard-induced vesication in isolated perfused porcine skin. Microsc Res Tech 1997; 37(3):229-241.

(16) Simon SR. Oxidants, metalloproteases and serine proteases in inflammation. Agents Actions Suppl 1993; 42:27-37.

(17) Holleran WM, Galardy RE, Gao WN et al. Matrix metalloproteinase inhibitors reduce phorbol ester-induced cutaneous inflammation and hyperplasia. Arch Dermatol Res 1997; 289(3):138-144.

(18) Woessner JF, Jr., Dannenberg AM, Jr., Pula PJ et al. Extracellular collagenase, proteoglycanase and products of their activity, released in organ culture by intact dermal inflammatory lesions produced by sulfur mustard. J Invest Dermatol 1990; 95(6):717-726.

(19) Lindsay CD, Rice P. Assessment of the biochemical effects of percutaneous exposure of sulphur mustard in an in vitro human skin system. Hum Exp Toxicol 1996; 15(3):237-244.

(20) Arbiser JL, Fan CY, Su X et al. Involvement of p53 and p16 tumor suppressor genes in recessive dystrophic epidermolysis bullosa-associated squamous cell carcinoma. J Invest Dermatol 2004; 123(4):788-790.

(21) Collier IE, Wilhelm SM, Eisen AZ et al. H-ras oncogene-transformed human bronchial epithelial cells (TBE-1) secrete a single metalloprotease capable of degrading basement membrane collagen. J Biol Chem 1988; 263(14):6579-6587.

(22) Bauer JW, Laimer M. Gene therapy of epidermolysis bullosa. Expert Opin Biol Ther 2004; 4(9):1435-1443.

(23) Cowan FM, Broomfield CA, Smith WJ. Exposure of human epidermal keratinocyte cell cultures to sulfur mustard promotes binding of complement C1q: implications for toxicity and medical countermeasures. J Appl Toxicol 2000; 20 Suppl 1:S77-S80.

(24) Powers JC, Kam CM, Ricketts KM et al. Cutaneous protease activity in the mouse ear vesicant model. J Appl Toxicol 2000; 20 Suppl 1:S177-S182.

(25) Casillas RP, Kiser RC, Truxall JA et al. Therapeutic approaches to dermatotoxicity by sulfur mustard. I. Modulaton of sulfur mustard-induced cutaneous injury in the mouse ear vesicant model. J Appl Toxicol 2000; 20 Suppl 1:S145-S151.

(26) Hager B, Bickenbach JR, Fleckman P. Long-term culture of murine epidermal keratinocytes. J Invest Dermatol 1999; 112(6):971-976.

(27) Pirrone A, Hager B, Fleckman P. Primary mouse keratinocyte culture. Methods Mol Biol 2005; 289:3-14.

(28) Niessen CM, Hogervorst F, Jaspars LH et al. The alpha 6 beta 4 integrin is a receptor for both laminin and kalinin. Exp Cell Res 1994; 211(2):360-367.

(29) Jones JC, Hopkinson SB, Goldfinger LE. Structure and assembly of hemidesmosomes. Bioessays 1998; 20(6):488-494.

(30) Rousselle P, Keene DR, Ruggiero F et al. Laminin 5 binds the NC-1 domain of type VII collagen. J Cell Biol 1997; 138(3):719-728.

(31) Pyke C, Romer J, Kallunki P et al. The gamma 2 chain of kalinin/laminin 5 is preferentially expressed in invading malignant cells in human cancers. Am J Pathol 1994; 145(4):782-791.

(32) Pyke C, Salo S, Ralfkiaer E et al. Laminin-5 is a marker of invading cancer cells in some human carcinomas and is coexpressed with the receptor for urokinase plasminogen activator in budding cancer cells in colon adenocarcinomas. Cancer Res 1995; 55(18):4132-4139.

(33) Kikkawa Y, Umeda M, Miyazaki K. Marked stimulation of cell adhesion and motility by ladsin, a laminin-like scatter factor. J Biochem (Tokyo) 1994; 116(4):862-869.

(34) Kikkawa Y, Akaogi K, Mizushima H et al. Stimulation of endothelial cell migration in culture by ladsin, a laminin-5-like cell adhesion protein. In Vitro Cell Dev Biol Anim 1996; 32(1):46-52.

(35) Symington BE, Carter WG. Modulation of epidermal differentiation by epiligrin and integrin alpha 3 beta 1. J Cell Sci 1995; 108 (Pt 2):831-838.

(36) Katayama M, Sekiguchi K. Laminin-5 in epithelial tumour invasion. J Mol Histol 2004; 35(3):277-286.

(37) Koshikawa N, Moriyama K, Takamura H et al. Overexpression of laminin gamma2 chain monomer in invading gastric carcinoma cells. Cancer Res 1999; 59(21):5596-5601.

(38) Pirila E, Sharabi A, Salo T et al. Matrix metalloproteinases process the laminin-5 gamma 2-chain and regulate epithelial cell migration. Biochem Biophys Res Commun 2003; 303(4):1012-1017.

(39) Schenk S, Hintermann E, Bilban M et al. Binding to EGF receptor of a laminin-5 EGF-like fragment liberated during MMP-dependent mammary gland involution. J Cell Biol 2003; 161(1):197-209.

(40) Balali-Mood M, Hefazi M. Comparison of early and late toxic effects of sulfur mustard in Iranian veterans. Basic Clin Pharmacol Toxicol 2006; 99(4):273-282.

(41) Shakarjian MP, Bhatt P, Gordon MK et al. Preferential expression of matrix metalloproteinase-9 in mouse skin after sulfur mustard exposure. J Appl Toxicol 2006; 26(3):239-246.

(42) Cowan FM, Broomfield CA, Smith WJ. Suppression of sulfur mustard-increased IL-8 in human keratinocyte cell cultures by serine protease inhibitors: implications for toxicity and medical countermeasures. Cell Biol Toxicol 2002; 18(3):175-180.

(43) Sabourin CL, Danne MM, Buxton KL et al. Cytokine, chemokine, and matrix metalloproteinase response after sulfur mustard injury to weanling pig skin. J Biochem Mol Toxicol 2002; 16(6):263-272.

(44) Smith KJ, Casillas R, Graham J et al. Histopathologic features seen with different animal models following cutaneous sulfur mustard exposure. J Dermatol Sci 1997; 14(2):126-135.

(45) Salo T, Kainulainen T, Parikka M et al. Expression of laminin-5 in ameloblastomas and human fetal teeth. J Oral Pathol Med 1999; 28(8):337-342.

(46) Opdenakker G, Van den Steen PE, Dubois B et al. Gelatinase B functions as regulator and effector in leukocyte biology. J Leukoc Biol 2001; 69(6):851-859.

(47) Yu Q, Stamenkovic I. Cell surface-localized matrix metalloproteinase-9 proteolytically activates TGF-beta and promotes tumor invasion and angiogenesis. Genes Dev 2000; 14(2):163-176.

(48) Liu Z, Shipley JM, Vu TH et al. Gelatinase B-deficient mice are resistant to experimental bullous pemphigoid. J Exp Med 1998; 188(3):475-482.